Next Research 2 (2025) 100288

Contents lists available at ScienceDirect

Next Research

journal homepage: www.elsevier.com/locate/nexres

Enhanced load frequency control in multi-source power systems with stochastic optimization algorithms and SMES integration via AC-DC parallel tie-lines

Md. Shahan Sarker[a], Md. Imtiaz Ahmed[a], Md. Alamgir Hossain[b], Md. Rashidul Islam[a,c,*], Md. Arafat Hossain[a], Md. Rafiqul Islam Sheikh[a]

[a] Department of Electrical and Electronic Engineering, Rajshahi University of Engineering & Technology, Rajshahi 6204, Bangladesh
[b] Queensland Micro-and Nano-Technology Centre, Queensland, 4111, Australia
[c] School of Electrical and Data Engineering, University of Technology Sydney, Ultimo, NSW 2007, Australia

ARTICLE INFO

Keywords:
Load frequency control
Automatic generation control
Renewable energy
Stochastic optimization algorithms
Proportional-integral-derivative control
Superconducting energy storage systems

ABSTRACT

The integration of renewable energy sources alongside conventional generators introduces challenges in maintaining frequency and power exchange between interconnected regions. To address these complexities and adjust the control parameters, this study investigates the application of three different stochastic optimization algorithms-particle swarm optimization (PSO), genetic algorithm (GA) and sine cosine algorithm (SCA)-combined with superconducting magnetic energy storage (SMES) technology for improved load frequency control (LFC). The results of integrating SMES technology are evaluated and compared with traditional control approaches in various operating scenarios. For the specific system with SMES, a single Proportional-Integral-Derivative (PID) controller was switched out for three PID controllers, and the results were noted for comparison. The expanded LFC technique effectively maintains optimal power exchange and a steady frequency throughout the linked regions, as demonstrated by the simulation results. This study bridges research gaps by combining advanced optimization algorithms and SMES technology to advance LFC, which is often overlooked in the literature. A comparative analysis under varying conditions confirms the effectiveness of the proposed system. The robustness of the system was validated with parameter variations of ±25 % and ±50 %, demonstrating its adaptability and reliability under dynamic conditions. When SMES was integrated, the deviation of the power of the tie line decreased by 13.59 %, the frequency deviation in area-1 improved by 34.13 %, and the frequency deviation of area-2 improved by 12.57 %. Therefore, the integration of SMES ensures dependable and sturdy performance in multiple power source systems linked by AC-DC parallel tie-lines. The results highlight the efficiency and resilience of the system, confirming its suitability for diverse operating scenarios.

1. Introduction

Power systems are rapidly evolving due to the integration of smart grid technologies and various renewable energy sources. An interconnected power system consists of components such as generation, transmission, distribution, and loads. In large interconnected networks, tie-lines link multiple service areas, which are geographically distributed. The growing size and complexity of power systems presents significant challenges in maintaining stability and reliability [1–4].

To maintain system stability, power generation must adapt to meet consumer demand. Any sudden increase in power demand can disturb the system's frequency and stability. This imbalance between power generation and consumption causes frequency fluctuations, which can cause instability and damage to electrical equipment [5–7]. To address these issues, it is essential to regulate energy production in each area to ensure balanced power exchange between interconnected regions [8].

The load frequency control (LFC) plays a key role in maintaining the system frequency and the power exchange between tie-line within acceptable limits. LFC uses a control loop to continuously adjust active power generation in order to maintain the system's frequency. Frequency control becomes even more complex in multi-area systems with diverse energy sources, such as thermal, hydro, wind, solar, gas, and nuclear energy [9,10].

Automatic Generation Control (AGC) is another important control system that ensures that frequency and power exchange remain at their desired levels. Ibraheem et al. [11] presents a comprehensive literature

* Corresponding author.
E-mail addresses: rashidul@eee.ruet.ac.bd, mdrashidul.islam@student.uts.edu.au (Md.R. Islam).

https://doi.org/10.1016/j.nexres.2025.100288
Received 4 October 2024; Received in revised form 21 March 2025; Accepted 24 March 2025

analysis that identifies AGC as a control system with three main goals:

1. Maintain the frequency of the system close to its assigned minimum value.
2. Enabling accurate power transfer between different areas.
3. Keeping optimal levels of generation levels to improve economic efficiency.

PID controllers are widely used for LFC due to their simplicity, cost-effectiveness, and reliability [12,13]. Advanced optimization techniques such as PSO, GA, and SCA further enhance their performance by optimally tuning gains to reduce frequency and tie-line power deviations [14,15].

Therefore, a control system is required to address the problem of unpredictable load alterations and to maintain the frequency at the desired levels. The design of the controller's precise tuning scheme plays an major role in providing optimal control. To efficiently control system frequency for single-area multi-source as well as two-area tie-line interconnected power systems (IPS), optimization techniques such as PSO, SCA and GA are applied to achieve better frequency and tie-line control. MATLAB/Simulink 2022b was used to develop the suggested power networks. By varying the system parameters in both networks by ±25 % and ±50 % and adjusting load in distinct scenarios for a double area tie-line power system, the proposed networks with PID were tested [16,17]. The gains of the PID controller were adjusted using PSO, SCA and GA approaches, with ITAE being the fitness function. In the suggested networks, the frequency responses, along with the power variations in the tie-line, were successfully optimized by the PID controller using PSO, SCA, and GA techniques. The following sections discuss the results of the PID controller and the optimization techniques we investigated and applied to the proposed networks.

1.1. Literature review

Significant research has been conducted in the LFC area to ensure the stability of the system, maintain the power flow of the tie-line within acceptable limits, and regulate the frequency of the system. Various methods have been proposed to address the challenges of maintaining system frequency and tie-line power flow at scheduled levels under minor disturbances and typical operating conditions. These solutions require robust control models with precise and fast responses to meet strict quality standards.

Intelligent controllers have made substantial progress in large-scale power systems, but challenges remain in their practical implementation. Modern control techniques for interconnected power systems are built on the foundational work of AGC and subsequent advances [18,19]. However, current power systems experience variable operating points and non-linear load characteristics [20], and studies addressing single-area or multi-area systems with or without high-voltage direct current(HVDC) links remain limited [21]. The Jaya-ITDF control strategy and the HVDC-link storage approach have been explored as effective solutions to improve frequency regulation in microgrid systems [22].

The integration of renewable energy sources and distributed generation has made the stability of the power system increasingly critical due to dynamic load variations [23]. Traditional fixed controllers often struggle to adapt to these dynamic conditions. LFC plays a crucial role in maintaining the real-time balance between power generation and load demand. LFC failures can cause frequency deviations, load imbalances, transmission delays, and sampling period problems [24].

The reviewed literature highlights the importance of optimization techniques and advanced secondary controllers to address these challenges. Oscillations caused by unpredictable load demands degrade power system performance, emphasizing the need for optimization approaches to improve system gains under varying conditions. A summary of the reviewed literature and its contributions is presented in Table 1.

To maintain tie-line power and frequency of the in their rated values, various soft computing-based control strategies have been developed in recent years. Table 1 presents the relevant literature related to this study, highlighting the number of approaches used to configure the gain in the PID controller and the Superconducting Magnetic Energy Storage (SMES) storage system. Many studies have focused on tuning the gain of the controllers. However, most of the existing work lacks a detailed comparison with other techniques, scalability to larger systems, and integration with modern renewable technologies. They often do not explore the robustness and stability of the system under dynamic conditions, such as parameter variations and fluctuating loads.

This study addresses these gaps by advancing LFC in multi-source power systems using stochastic optimization algorithms, such as PSO, GA, and SCA,which have been widely used to optimize controller parameters. The ITAE (Integral of Time-weighted Absolute Error) objective function is selected for a comprehensive performance evaluation. The integration of SMES improves frequency regulation and system stability, addressing challenges posed by dynamic load variations and integration of renewable energy.

A comparative analysis of PSO, GA, and SCA for PID tuning demonstrates that GA-PID controllers outperform others in minimizing overshoot, undershoot, steady-state error, and settling time. Additionally, the integration of SMES and AC-DC parallel tie-lines significantly improves the robustness of the system. The study evaluates single versus multiple PID controllers to optimize interconnected systems effectively.

A rigorous time-domain stability analysis using MATLAB/SIMULINK validates system performance under dynamic conditions. Key performance metrics-frequency deviation, power deviations, and settling times-highlight the superiority of the GA-PID controller configuration. The stability and robustness of the system are tested under varying parameters and load changes, demonstrating substantial improvements in performance and reliability.

The primary objective of this research is to improve the effectiveness of LFC and ensure network stability under challenging conditions, ultimately providing high-quality power to all consumers. The results offer valuable insights into improving modern multi-source power systems through optimized control strategies.

1.2. Major contributions and highlights

This study focuses on LFC in IPS with dual-area tie-line networks and single-area, multi-source energy systems comprising thermal, hydro and gas power plants. The proposed system is evaluated under varying system constraints and load conditions using the ITAE objective function, demonstrating the effectiveness of tuned controllers. The work addresses the critical need for the stability of the power system amid dynamic load changes and integration of renewable energy, where traditional controllers often fail.

The research highlights a thorough comparison of three optimization algorithms: PSO, GA and SCA. GA shows remarkable performance in minimizing errors and achieving faster settling times. The integration of SMES, alongside AC-DC parallel tie-lines, significantly improves frequency regulation and system stability, offering a robust solution for modern multi-source power systems. The key contributions of this study are summarized as follows:

- **Integration of multiple energy sources:** A model incorporating thermal, hydro, and gas power plants to address variability in renewable energy.
- **Integration of SMES:** This research addresses the successful integration of SMES and its exceptional performance in this specific system configuration.
- **Advanced control strategies:** To accomplish these improvements, this study uses stochastic optimization algorithms (GA, SCA, and PSO) in conjunction with ITAE as the objective function.

Table 1
Review of studied literature.

Optimization approach	Secondary controller	Main contribution	Drawback	Reference
Snake Optimizer (SO)	PID	Uses Snake Optimizer for PID tuning in a diesel-wind hybrid system for frequency regulation, integrating UC and RFB for improved performance.	Limited to diesel-wind systems; lacks real-time optimization and broader energy storage analysis.	[36]
PSO	AGC Tuning	Tunes AGC for interconnected reheat thermal systems using PSO for improved performance.	Lacks testing with renewable energy systems.	[37]
Differential Evolution (DE)	PID controller	Enhances AGC dynamic performance in two-area power systems using MATLAB-based analysis.	Lacks testing with modern renewable technologies.	[38]
DE	LFC Controller	Tunes LFC controller parameters using differential evolution algorithm for multi-source systems.	Lacks practical implementation validation.	[14]
GA	Hydro-Thermal Scheduling	Optimizes short-term hydro-thermal scheduling using random transfer vectors in GA.	Limited to short-term analysis and lacks renewable energy integration.	[39]
PSO-Scaled Fuzzy Logic	Hydro-Thermal Systems	Implements PSO-scaled fuzzy logic controller for LFC in hydro-thermal systems.	Limited analysis on renewable energy integration.	[40]
Gravitational search algorithm (GSA)	Model Predictive Controller (MPC)	Designs MPC for LFC in nonlinear multi-area systems with energy storage integration.	Lacks hybrid optimization techniques and experimental comparison.	[41]
Tilt Integral Derivative (TID)	Multi-Source Systems	Implements TID controller for two-area multi-source systems, improving LFC performance.	Lacks advanced energy storage system integration.	[42]
Multi-Verse Optimizer	Fuzzy-PID Controller	Develops multi-verse optimizer-based fuzzy-PID controller with derivative filter for LFC of multi-area systems.	Lacks detailed comparison with other optimization techniques.	[43]
Optimal Fuzzy-PID	UPFC and SMES	Proposes optimal fuzzy-PID with derivative filter for LFC including UPFC and SMES.	Lacks focus on hybrid optimization techniques and multi-area scalability.	[44]
Fractional Order Cascade Controller	HVDC Tie-Link	Proposes a novel fractional-order cascade controller for AGC using HVDC tie-links in restructured power systems.	Limited discussion on renewable integration and storage systems.	[45]
Multi-Verse Optimizer	Model Predictive Controller	Proposes a multi-verse optimizer-based MPC for LFC in hybrid multi-interconnected plants with renewable energy.	Lacks discussion on dynamic load variations and energy storage scalability.	[46]
Neuro-Fuzzy Logic	Parallel Resonance BFCL	Improves fault ride-through capability of DFIG-based wind farms using neuro-fuzzy logic-based fault current limiter.	Limited to wind systems; lacks broader application.	[47]
Water Cycle Algorithm	Type-II Fuzzy Controller	Proposes WCA-optimized fuzzy controller for multi-area multi-fuel systems considering communication delays.	Lacks real-time validation and hybrid renewable integration.	[48]
Salp Swarm Algorithm (SSA)	PID	Proposes SSA-based PID controller optimized with energy storage devices (BESS, FESS, UC) for improved LFC performance and stability.	Limited to small-scale systems; lacks comparison with hybrid algorithms and exploration of dynamic load variations.	[49]
Hybrid GA-PSO	PID Controller	Combines GA and PSO for LFC in multi-area power systems, improving convergence and system stability.	Requires deeper analysis of computational complexity and real-world scalability.	[50]
SSA	Fuzzy 1PD-PI	Proposes SSA-optimized fuzzy 1PD-PI controller for AGC in renewable-assisted thermal and hydro-thermal systems.	Limited to single and two-area systems; lacks comparison with other metaheuristics and advanced energy storage systems.	[51]
SSA	Fuzzy 1PD-TI	Proposes SSA-optimized fuzzy 1PD-TI controller for AGC in multi-source systems with renewable energy and storage devices.	Lacks comparison with other stochastic techniques, scalability to larger systems, and detailed modeling of hybrid storage systems.	[52]
Twin Delayed DDPG	DRL-based Controller	Efficient LFC for renewable-integrated power systems using deep reinforcement learning.	Lacks cost analysis and testing in larger multi-area systems.	[53]
Optimal Neural Network	Load Frequency Controller	Designs an optimal neural network-based controller for improved LFC performance.	Limited scalability and lacks hybrid storage integration.	[54]
Optimization Techniques (GA, PSO, AI)	AGC/LFC Strategies	Reviews advancements in AGC/LFC with focus on optimization techniques, renewable integration, and multi-area systems.	Lacks exploration of energy storage systems, hybrid optimization methods, and experimental validation.	[55]
Modified SCA	PID/Fuzzy-PID Controllers	Designs optimal PID/Fuzzy-PID controllers for AGC in deregulated power systems using modified SCA, improving system stability and dynamic response.	Limited validation on large-scale, real-time systems.	[56]
Hybrid Crow Search Algorithm (HCSA)	Cascaded PI-PIDN	Proposes cascaded PI-PIDN controller optimized with HCSA for LFC in a three-area system with RES and ESS integration.	Lacks comparison with recent metaheuristic algorithms and broader system configurations for robustness testing.	[57]
Artificial Rabbit Optimization (ARO)	FOPD Cascade Controller	Proposes an FOPD cascade controller optimized with ARO for multi-area renewable-integrated hydro-thermal systems with redox flow battery storage.	Lacks comparison with alternative optimization techniques and integration of other ESS like SMES. Limited discussion on real-world implementation and hybrid optimization strategies.	[58]
Emperor Penguin Optimizer (EPO)	TI-FOIDN Cascade Controller	Proposes TI-FOIDN cascade controller optimized with EPO for optimal FACTs device placement in LFC, validated using RT-Lab simulations.	Lacks comparison with other metaheuristic algorithms and scalability analysis for large multi-area systems. Limited real-world deployment discussion.	[59]
Crow Search Algorithm (CSA)	Cascade FOPDN-FOPIDN Controller	Proposes a CSA-optimized cascade FOPDN-FOPIDN controller for AGC with improved real-time performance validated using the novel HPA-ISE index.	Lacks comparison with other metaheuristic methods, scalability for large grids, and integration with renewable energy sources.	[60]
Robust Neural Controllers	Neural Network-Based PID	Proposes robust neural controllers for power systems using new reduced models and validates their performance on test systems.	Lacks scalability analysis and comparison with other advanced AI-based techniques.	[61]

(*continued on next page*)

Table 1 (*continued*)

Optimization approach	Secondary controller	Main contribution	Drawback	Reference
RT-Lab with EPO Optimization	FOPI-TIDN	Proposes FOPI-TIDN controller optimized by emperor penguin optimizer (EPO) in AGC with SMES-IPFC integration under deregulated environments.	Lacks detailed market analysis, benchmarking with hybrid metaheuristics, and generalization to larger systems.	[62]
Snake Optimizer (co-SO)	EXP-PID	Proposes EXP-PID controller with nonlinear features and validated using snake optimizer on test scenarios.	Lacks comparison with hybrid techniques and scalability for larger systems.	[63]
Solar PV with Energy Storage	SFS-PIDDμ	Proposes PIDDμ controller with fractional derivative optimized by SFS; integrates Solar PV, BESS, and FESS for improved LFC.	No comparison with hybrid techniques; lacks multi-area scalability and long-term cost analysis.	[64]
TSA Optimizer (TSA)	PDN (FOPI) Controller	Proposes TSA-optimized PDN (FOPI) controller for AGC in hybrid hydrogen electrolyser-fuel cell and redox-flow battery systems, ensuring flexibility and reliability.	Lacks comparison with other storage solutions, long-term performance evaluation, and renewable energy integration.	[65]
Reinforcement Learning (RL)	RL-based Controller	Develops RL-based LFC approach for power systems with high renewable penetration, demonstrating adaptability and robustness.	Requires more real-time validation and consideration of large-scale system complexities.	[66]
Hybrid Aquila Arithmetic Optimization	ANFIS	Mitigates harmonic issues in grid-connected solar systems using hybrid ANFIS.	Limited scalability to large systems and other renewable integrations.	[67]
PSO and GA Algorithms	PID Controller	Proposes optimized PID controllers using PSO and GA algorithms for effective LFC in dual-area multi-source power systems.	Limited validation for real-time implementation in large-scale systems.	[68]
Firefly Algorithm (FA)	Integral-Derivative Controller	Applies Firefly Algorithm for controller optimization, improving frequency stabilization in LFC systems.	Sensitivity to initialization and slower convergence.	[69]
Artificial Bee Colony (ABC)	PID Controller	Uses ABC algorithm to optimize PID controllers, achieving faster settling time and reduced frequency deviations.	Limited comparative analysis with other metaheuristic methods.	[70]
Tidal turbine aids microgrid frequency regulation via a novel cascade Fuzzy-FOPID droop in the de-loaded region	Cascade Fuzzy-FOPID droop control	Proposes a novel cascade Fuzzy-FOPID droop control strategy for tidal turbines operating in the de-loaded region to support microgrid frequency regulation.	Limited to simulation studies; lacks experimental validation.	[71]
Barnacle Mating Optimizer (BMO)	Frequency stabilization in Multi-Microgrid using Barnacle Mating Optimizer-based cascade controllers	Introduces a cascade controller optimized using the BMO algorithm for frequency stabilization in a multi-microgrid system.	Focuses primarily on algorithmic development; practical implementation aspects are not thoroughly discussed.	[72]
FOPTID+1 controller with capacitive storage enhances AGC in multi-source power systems	Fractional Order Proportional-Integral-Derivative Plus One (FOPTID+1) controller	Enhances Automatic Generation Control (AGC) performance by integrating a FOPTID+1 controller with capacitive energy storage in multi-source power systems.	The study is primarily theoretical; real-world applicability needs further exploration.	[73]

- **Comparison of PID controllers:** Insights into the performance of three PID controllers versus a single PID controller, demonstrating the superior effectiveness of multiple controllers.
- **Robust performance:** The proposed system maintains stability and reduces steady-state errors under varying loads and constraints.
- **Stability analysis:** Time-domain stability analysis is conducted using MATLAB/SIMULINK to evaluate the proposed control strategy. The controller gains and SMES parameters are tuned for optimal performance, and the step responses of frequency and power deviations in the two-area power system with SMES integration are analyzed.
- **Practical implications:** Resilient power networks with enhanced stability, efficiency, and adaptability.

The study reveals that the configuration with three GA-PID controllers and SMES delivers superior performance, minimizing steady-state error, undershoot, overshoot, and settling time, proving its effectiveness and reliability.

1.3. Structure of the article

This article is formatted as follows: a comprehensive study of the literature is done in Section 1, where several controller optimization methodologies are explored, and the power system under investigation is thoroughly analyzed, with its numerous components and complexities explained. A description of the control approach, which uses stochastic optimization methods that include PSO, GA, and SCA, is provided in Section 2. In Section 3, the problem of mulation is covered in detail, together with an outline of the main parameters and constraints and an explanation of the objective functions that will guide the investigation. The simulation results are thoroughly reported in Section 4, which also provides an analysis of the work for various optimization techniques and evaluates the effectiveness of the suggested solution. This involves investigating multi-area multisource power systems with and without SMES, evaluating different stochastic optimization techniques, and looking at scenarios involving one or three PID controllers. In this section, the robustness and stability of the proposed system are also analyzed. Section 5 concludes with a summary of the contributions and implications of the investigation, based on the key results of the study.

2. Methodology

Stochastic optimization techniques of various types are used to enhance the LFC and AGC of two-area power systems connected by parallel AC-DC tie-lines. The system model and the traditional two-area scheme are thoroughly explained in the next subsections. Describes the benefits and in-depth idea of SMES. The section on AC-DC parallel tie-lines discusses how well tie-lines work in a system. It also uses mathematical equations to demonstrate the general idea of a PID controller. It

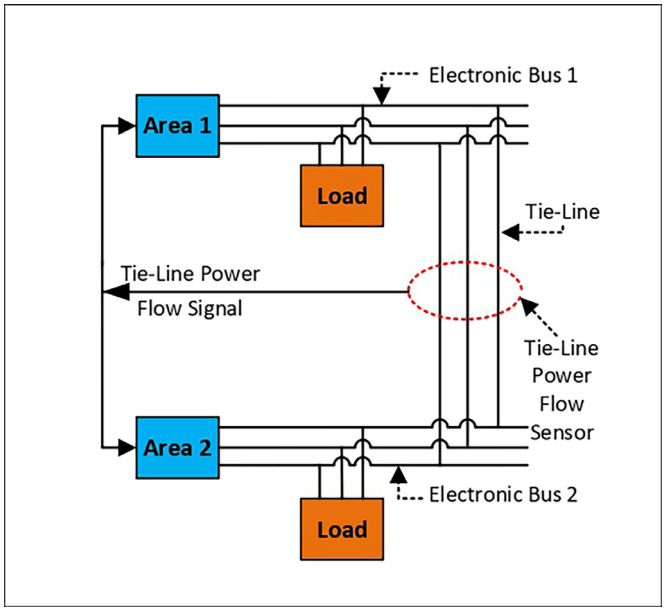

Fig. 1. Traditional dual-zone setup: fundamental block schematic illustration.

makes use of flowcharts and descriptions of certain stochastic optimization techniques (PSO, GA, SCA).

2.1. System description

The approach uses a multi-source power system that includes renewable energy sources and conventional generators in each region with small and medium-sized enterprises. Moreover, the system allows connections to be established via AC-DC parallel ties, as Fig. 1 illustrates.

2.1.1. Model for load frequency control

The dynamic equations for the frequency variations, tie-line power flow, and two-area power system are included in the formulation of the LFC. Two single areas joined by a power connection known as the "tie line" constitute a two-area system. Electric power interchange occurs between regions facilitated by the tie-line, while each region independently supplies electricity to its consumers from locally generated sources. The interconnection via the tie-line introduces a dynamic interdependence such that a load disturbance in one region affects both the power flow on the tie-line, as shown in Fig. 2, and the output frequencies of both regions. In order to restore the local frequency to its steady state value, the control system in each region requires information about the transient conditions in both regions. The fluctuation in the output frequency in a specific region, as documented in Hakimuddin et al. [25], serves as an informative indicator of the dynamic state of the local area.

2.1.2. HVDC link multi-source multi-area power system

Two region power system modeling is done with MATLAB Simulink, which is connected by parallel AC-DC tie-lines and consists of a more realistic combination of generating units, including gas, hydro, and reheat thermal units in every region. Furthermore, not all the generators in a given area will participate in the LFC job, and the rates of involvement vary between the participating generators. The total participation factor of all generators involved in a control region is equal to unity Fig. 3 shows the transfer function model of a multi-source, multiarea system with an HVDC connection and integral controllers.

2.1.3. SMES system: superconducting magnetic energy storage

Superconducting coils are used in SMES, an advanced energy storage technique, to store electrical energy as a magnetic field. It is used in AGC for two-area power systems in power systems [26,27]. AGC benefits from utilizing SMES in several ways.

1. The superconducting coils can release or absorb energy rapidly, providing fast frequency regulation and damping of power oscillations.
2. SMES systems have a high energy storage density compared to conventional energy storage technologies.
3. SMES systems have a long operational life with minimal degradation.
4. The rapid response of the SMES systems helps regulate the frequency of the system, ensuring that it remains within acceptable limits.

2.1.4. AC-DC parallel tie-lines

For AGC, power exchange and system stability are maintained between the two locations by the use of AC-DC parallel tie-lines, which permit power flow in both AC and DC versions. The following describes the use of AC-DC parallel tie-lines for AGC in a two-area power system:

- Real-time data interchange occurs between the two sectors via the AC-DC tie-lines,
- Through the AC-DC tie-lines, the AGC controllers in both zones share pertinent information and control signals,
- This tie-line is used to manage power flow,
- This tie-line is used by the AGC controllers to continually check the frequency variations in both locations,
- In the event of sudden changes in generation or load, it helps maintain system stability.

However, advanced control and real-time monitoring strategies are essential for effective AGC and power exchange in such systems.

2.2. Control strategy with stochastic optimization algorithms

In a two-area power system, the use of stochastic optimization techniques for AGC can offer reliable and effective control methods that can adapt to changing and unpredictable conditions. Stochastic optimization algorithms are methods to solve complicated and uncertain optimization issues because they incorporate randomness or probabilistic aspects. This is a control scheme for an AGC in a two-area power system that uses stochastic optimization methods. Mention the control goal, which is to use PSO, GA, and SCA algorithms to reduce the frequency deviations and power variations of the tie-line.

2.2.1. PID controller: proportional-integral-derivative approach

When creating a controller, its primary function needs to be taken into account above anything else. This might include the following: absorption of load disturbances, sensitivity to measurement noise, robustness to model uncertainty, and ability to follow the set point. The widely utilized and well-liked PID feedback controller is found in many contemporary sectors. PID controllers are widely used in many different single-input, single-output applications, which contributes to their popularity. PID controllers are frequently utilized when quick reaction times and stability are needed. For multi-source, multi-area realistic power systems, it is reported in Mohanty et al. [28] that the DE-tuned PID controller performs better than the DE-tuned PI and I controllers. Given the foregoing considerations, the present study employs the PID controller to evaluate and compare the performance of analogous power systems.

The dynamic behavior of the PID controller in the Laplace domain is captured by the transfer function $G_{\mathrm{PID}}(s)$.

Here is how the transfer function is derived. The difference between the intended set point $r(t)$ and the actual output $y(t)$ is the error signal $e(t)$ to be considered.

$$e(t) = r(t) - y(t) \tag{1}$$

The proportional term contributes to the control effort in proportion to the current error:

$$u_P(t) = K_p \cdot e(t) \tag{2}$$

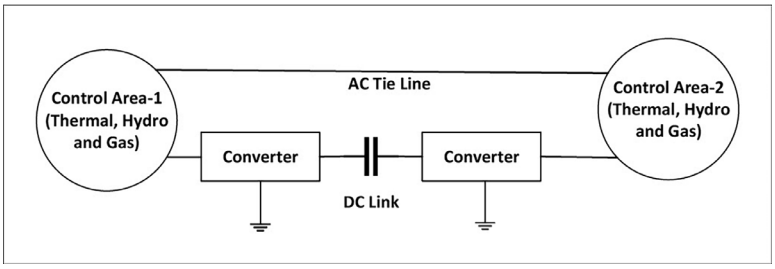

Fig. 2. Parallel AC-DC tie-lines connect two region power systems.

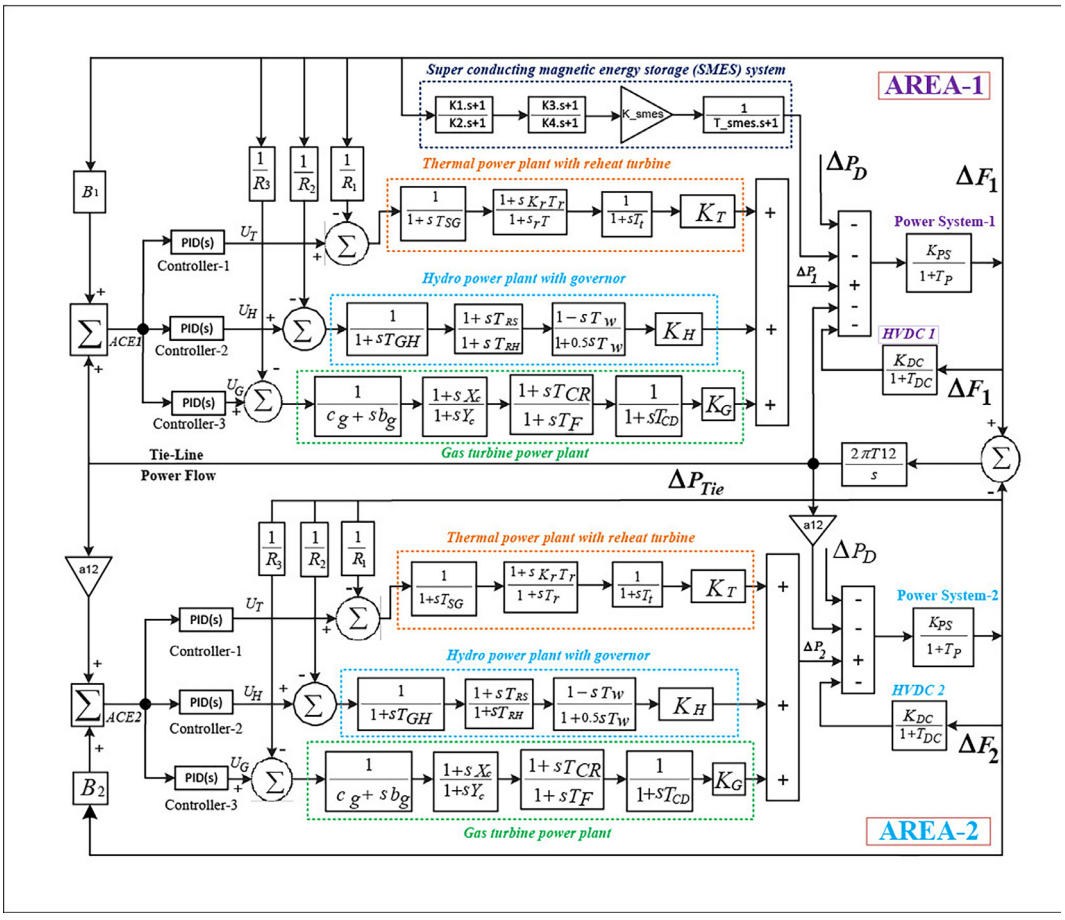

Fig. 3. Two-area power systems with SMES.

The integral term accumulates the past errors to eliminate steady-state errors:

$$u_I(t) = K_i \int_0^t e(\tau)d\tau \tag{3}$$

The derivative term uses the current error's rate of change to predict future errors:

$$u_D(t) = K_d \frac{de(t)}{dt} \tag{4}$$

The total control effort $u(t)$ is the sum of these three terms:

$$u(t) = u_P(t) + u_I(t) + u_D(t) \tag{5}$$

Taking the Laplace transform of $u(t)$ and $e(t)$ gives us:

$$U(s) = K_p E(s) + \frac{K_i}{s} E(s) + K_d s E(s) \tag{6}$$

Solving for the transfer function $G_{\text{PID}}(s) = \frac{U(s)}{E(s)}$, we get:

$$G_{\text{PID}}(s) = K_p + \frac{K_i}{s} + K_d s \tag{7}$$

where, $G_{\text{PID}}(s)$, the PID controller transfer function; K_p, benefit proportionate to; K_i, gain integral; K_d, gain on derivative; s, complex frequency variable.

The proportional (P), integral (I) and derivative (D) terms combine to form the transfer function of a PID controller. In the Laplace domain, the dynamic behavior of the PID controller is captured by the transfer function $G_{\text{PID}}(s)$.

2.2.2. Particle swarm optimization (PSO)

Fish schools and flocks of birds serve as models for the social behavior of PSO, a stochastic optimization algorithm. Kennedy and Eberhart presented it in 1995. A computational methodology aimed at iteratively refining a candidate solution is used to maximize a predetermined quality metric. This approach involves a population of potential solutions, denoted as particles, which are systematically manipulated within the search space. The manipulation is governed by a straightforward mathematical formula that regulates both the particle's position and velocity. Currently, as alternative particles identify improved locations within

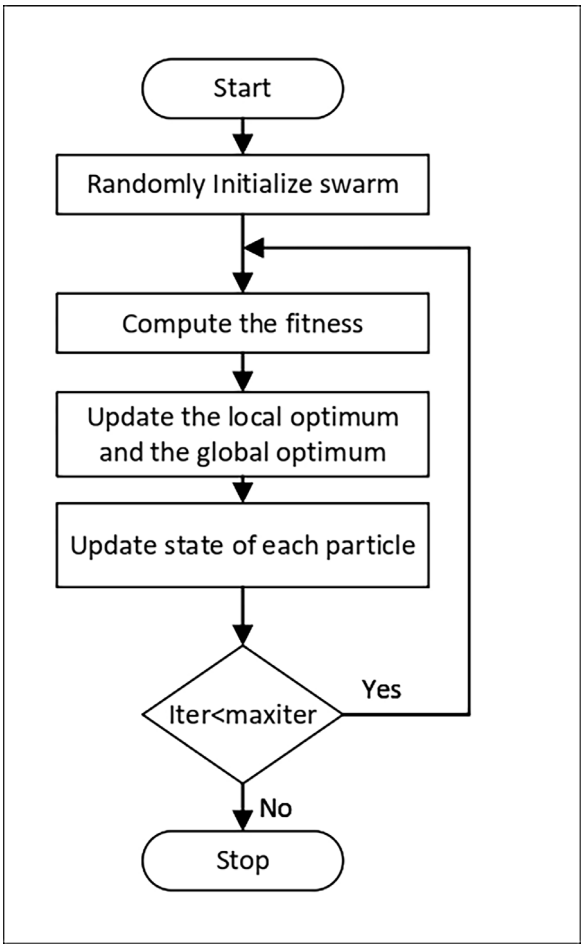

Fig. 4. An illustration of the fundamental PSO algorithm.

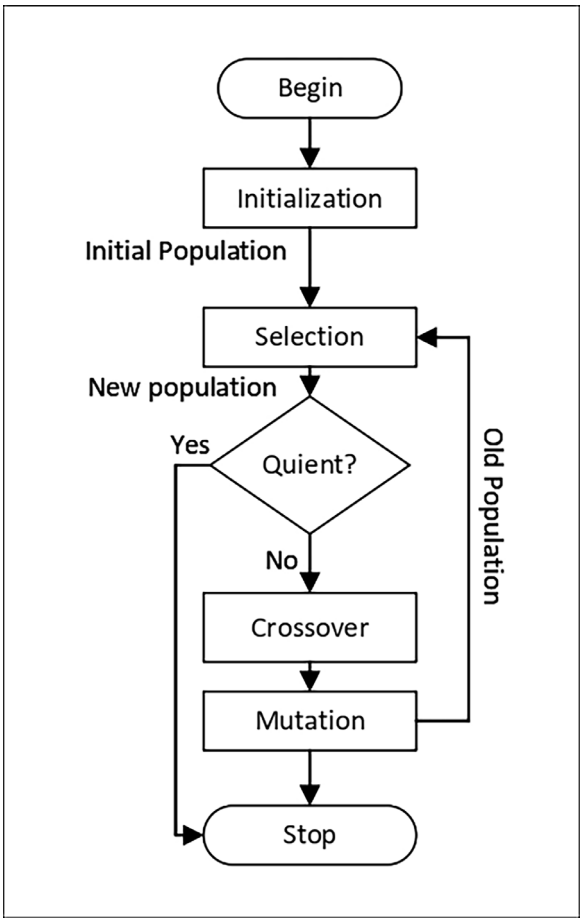

Fig. 5. Flowchart for basic GA.

the search space, each particle is directed toward these newly identified optimal positions, supplementing its pursuit of the locally recognized optimum. As a result, the swarm should be directed toward the optimal solutions shown in Fig. 4. Function optimization, neural network training, control system tuning, feature selection in machine learning, image processing, data clustering, and other optimization issues are among the many PSOs used for [29].

In general, PSO is a versatile and efficient optimization algorithm with many practical applications due to its simplicity and effectiveness in finding near-optimal solutions in a wide range of problem domains.

2.2.3. Genetic algorithm (GA)

The natural selection and evolution theories provide the foundation for GA, an optimization method inspired by nature. Since John Holland first presented it in the 1970s, it has gained popularity as a technique for resolving challenging optimization issues. Better solutions evolve over generations as a result of individuals with higher fitness having a higher probability of surviving and reproducing, a process that the GA simulates. The natural selection process that GA, a metaheuristic, uses is a component of the evolutionary algorithm (EA). The three biological operators shown in Fig. 5 that produce high-quality solutions to optimization and search problems are mutation, crossover, and selection. A standard genetic algorithm needs the following:

- The genetic representation of the solution domain.
- A fitness function to assess the solution domain.

Widely used in a variety of optimization problems, GA finds extensive application in Srinivas and Patnaik [30], Abeg et al. [31], function optimization, traveling salesman problem (TSP), knapsack problem, scheduling and time-tabling problems, parameter tuning in machine learning algorithms, and engineering design optimization.

In general, GA is a powerful optimization technique that can efficiently explore complex solution spaces and find near-optimal solutions in a wide range of problem domains.

2.2.4. Sine cosine algorithm (SCA)

In 2016, Mirjalili unveiled the SCA, an optimization algorithm inspired by nature. It is intended to resolve continuous optimization issues and draws inspiration from sine and cosine functions. SCA is a straightforward yet effective algorithm that explores the search space by imitating the periodic movement of the sine and cosine functions. SCA is a cutting-edge optimization technique for handling optimization problems. It creates a number of initial random candidate solutions using a mathematical model based on sine and cosine functions and drives them to vary either outwards or towards the optimal solution. This method also incorporates a number of adaptive and random variables to highlight search space exploration and exploitation at various optimization milestones, as seen in Fig. 6. Function optimization, engineering design optimization, feature selection in data mining, feature tuning in machine learning methods, image processing, neural network training, and other optimization issues have all seen the use of the SCA [32].

All things considered, the SCA is a promising optimization method, particularly for issues involving continuous optimization. It performs competitively compared to other metaheuristic algorithms in a variety of real-world situations and provides simplicity and speed. However, the exact situation at hand will determine which method is best, and this may need some trial and error as well as comparison shopping with other optimization strategies.

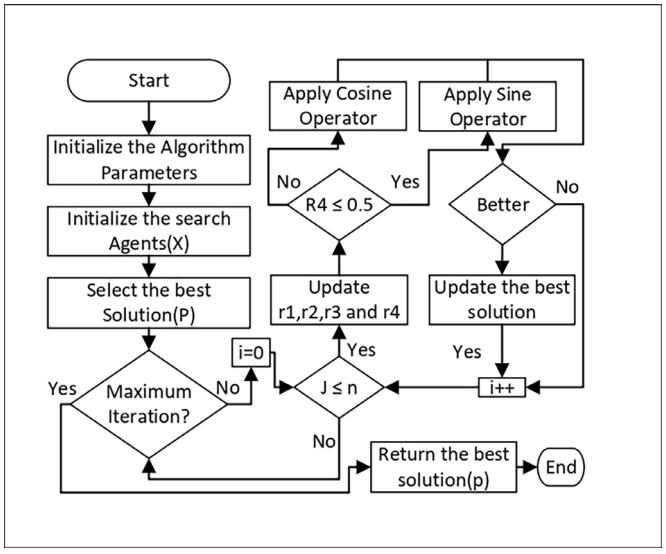

Fig. 6. Flowchart for basic SCA algorithm.

2.2.5. Optimization implementation

This case applies the PSO, GA, and SCA algorithms for LFC in the multi-source power system. Here, we develop the algorithm-specific parameter and convergence criterion initialization process for each algorithm's integration with the LFC model.

3. Problem formulation and objective functions developments

The ITAE objective function serves as a crucial performance metric within control systems. Measures the accumulated error between the desired system response and the actual response over a specific duration. By minimizing the ITAE value, the controlled system is able to advance closely and quickly, adhering to the intended behavior. Performance requirements for control system design frequently make use of the integral of absolute error (IAE). Although ITAE and IAE are used in different control scenarios, ITAE is used more frequently in research related to AGC. This preference results from the fact that systems with ITAE as their goal function typically settle faster. As a result, as stated in Barisal [33], the ITAE objective function has been particularly selected. Moreover, the goal function definition for a multi-source power system is specified using the formulation given in Mohapatra et al. [34].

$$J = ITAE = \int_0^{t_{\text{sim}}} (|\Delta F_1|) + (|\Delta F_2|) + (|\Delta P_{\text{Tie}}|) \cdot t \, dt \tag{8}$$

where ΔF_1 and ΔF_2 are the area-1 and area-2 frequency deviations, respectively, and J is the objective function. The simulation time range is t_{sim}, and the incremental change in the power tie-line is ΔP_{Tie}. Reduce J considering PID controller improvements, such as

$$K_{ij_{\min}} \le K_i \le K_{ij_{\max}}, \text{ where } i = P, I, D \text{ and } j = 1, 2, 3. \tag{9}$$

In this case, the control parameter for the (integral) component i is K_i. The controller settings have been set with a minimum value of -1 and a maximum value of 1, as documented in the literature. With the corresponding control inputs denoted U_T, U_H, and U_G, the differential equation of the PID controller for each of the thermal, hydro and gas units of the power system may be expressed as

$$U_T = K_{P1}\text{ACE1} + K_{I1} \int \text{ACE1} + K_{D1} \frac{d\text{ACE1}}{dt} \tag{10}$$

$$U_H = K_{P2}\text{ACE1} + K_{I2} \int \text{ACE1} + K_{D2} \frac{d\text{ACE1}}{dt} \tag{11}$$

$$U_G = K_{P3}\text{ACE1} + K_{I3} \int \text{ACE1} + K_{D3} \frac{d\text{ACE1}}{dt} \tag{12}$$

The ACE signal, along with the power error information from the connection line and the frequency error information, represents the area control error for a specific control area. One method of representing them may be [35]. Concerning area 1:

$$\text{ACE1} = B1 \cdot \Delta F_1 + \Delta P_{\text{Tie}} \tag{13}$$

For area-2:

$$\text{ACE2} = B2 \cdot \Delta F_2 - \Delta P_{\text{Tie}} \tag{14}$$

In this study, the differential evolution method, the PSO approach, and GA were used to analyze the LFC performance of the suggested system to determine the gain settings of the PID controller based on the accepted cost functions. To sum up, the control strategies that have been discussed entail modifying the amounts of power generation to keep the frequency of the system within reasonable bounds. In order to minimize the ITAE objective function, stochastic optimization methods such as PSO, GA, and SCA are used to maximize controller gains. The controllers can quickly adjust to system changes and uphold intended performance requirements thanks to these algorithms.

4. Results and analysis of simulations

The investigation used MATLAB (R2022b) on a personal computer equipped with an 8th generation Intel Core i5 CPU (3.4 GHz) and 8 GB of RAM. Using MATLAB/ SIMULINK, a comprehensive system model was constructed to elucidate the dynamic characteristics of the power system. The main goal was to identify the best performance of the controllers in improving automated load frequency control. PSO, GA, and SCA were used in optimization tasks using MATLAB scripts. Recurrent fine-tuning of PID controller settings was facilitated by these programs. Using certain initial gain scheduling settings, the model was simulated. The objective function, which measures the performance of the system under load frequency management, was calculated from the simulation output. Optimization techniques (PSO, GA, SCA) were influenced by objective function values to repeatedly optimize PID controller gains.

4.1. Performance analysis for different types of stochastic optimization algorithms

The main emphasis of this work was an integrated, multi-area, multi-source power system with integral controls, as shown in Fig. 3. The main goal was to determine the best control settings that would result in effective system operation. The study involved a thorough investigation of many situations related to a range of control parameters. Of particular importance was the accurate adjustment of settings for PID controllers and SMES integration. The core of the optimization process was the application of the ITAE objective function.

Fig. 3 is a graphic representation of the three different stochastic optimization methods (PSO, SCA, and GA) that are discussed in Section 2.1.2 and then used in this investigation. For every adjustment in the parameter values, a total of 50 separate runs were performed in order to offer a quantitative assessment of the results. Using optimized PSO, SCA and GA algorithms, the optimization process was performed fifty times.

The convergence curves portraying the ITAE objective function, as exemplified in Fig. 7, provide valuable information. In summary, the PSO algorithm demonstrates swift convergence, reaching a near-optimal state by the 5th iteration, with limited potential for further improvement even with an increased number of iterations. However, the SCA algorithm exhibits a moderate convergence rate, culminating in final convergence around the 34th iteration out of a total of 50 iterations. There exists the possibility of marginal reductions in the objective function with additional iterations, indicating a gradual refinement. In contrast, the GA algorithm converges at a notably slower pace, achieving a substantial reduction in the objective function relatively quickly. It reaches its ultimate convergence point around the 28th iteration of the

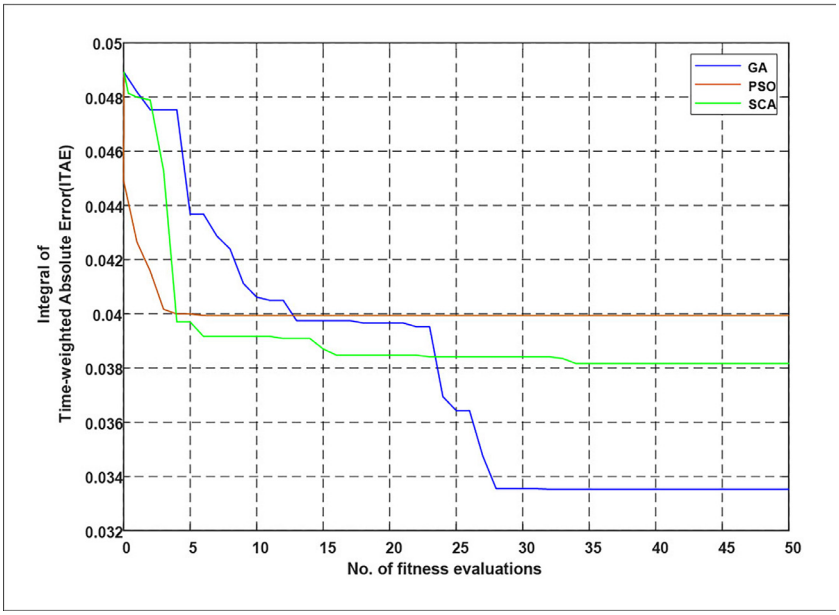

Fig. 7. Convergence curve for GA, PSO, and SCA algorithm.

Table 2
Interpretation and evaluation of several stochastic optimization techniques in multi-source power systems integrating SMES through AC-DC Parallel tie-lines.

Algorithm	Variance	Best value	Worst value	Average value	Mode
PSO	3.4658e−05	0.0227	0.0474	0.0334	0.0227
SCA	2.1890e−05	0.0159	0.0341	0.0224	0.0159
GA	**1.6004e − 05**	0.0141	0.0282	0.0222	0.0141

*Bold fonts indicate the minimum variance of the objective function value.

Table 3
GA with SMES integration via AC-DC parallel tie-lines yields tuning results for PID controllers and SMES parameters.

Parameters	Value
PID Controller- 1	K$p1$ = 8.745
	K$i1$ = 9.977
	K$d1$ = 5.747
PID Controller- 2	K$p2$ = 8.082
	K$i2$ = 0.0228
	K$d2$ = 2.463
PID Controller- 3	K$p3$ = 9.892
	K$i3$ = 8.028
	K$d3$ = 3.727
SMES	k1 = 8.818
	k2 = 4.935
	k3 = 0.905
	k4 = 5.927
	k_$smes$ = 9.824
	t_$smes$ = 4.200

total of 50. Its rigorous and thorough optimization process is highlighted by the possibility of further reductionsin objective functions with more iterations.

Several different mutation techniques were investigated and Table 2 carefully recorded the associated variance, average, best value, worst value, and mode ITAE values. The final goal was to determine the ideal value of the ITAE objective function, which would enable the identification of the method that provides the best tuning parameters for the three PID controllers and the integration of SMES. The goal of this thorough analysis was to determine the method that would improve the multi-source power system's overall performance by producing the best tuning parameters for the PID controllers and SMES integration in addition to producing the optimal objective function value of ITAE. The complex balancing of three PID controller parameters and SMES parameters is required for an ideal solution, which results in improved system performance based on predetermined parameters.

The solutions obtained from 50 iterations of the GA are rigorously evaluated. The final result is determined by selecting the iteration that most closely matches the predetermined criteria, as shown in Table 3. This specific solution offers an effective and efficient method of controlling the system by combining the ideal values of the SMES and PID controllers.

The effects on the system are observable through the careful selection of the most suitable parameters. Specifically, Fig. 8 illustrates the frequency fluctuations in Area-1 and Fig. 9 illustrates the frequency variations in Area-2. Furthermore, dynamic changes in the power of the tie-line are shown in Fig. 10, highlighting the importance of AC-DC parallel tie-lines in overall performance.

In conclusion, the statement outlines a procedure for using a GA to adjust the SMES and PID controller parameters. After 50 iterations of the algorithm to test several solutions, the best performing solution is selected as the ultimate and ideal result for system control.

The insights derived from this study contribute to the advancement of LFC strategies in complex power system configurations, facilitating enhanced stability and power exchange.

4.2. Multi-source power system in several areas, both with and without SMES

Instead of integrating SMES, we concentrated on a multi-area multi-source power system integrated with integral controllers, as shown in Fig. 3. Optimizing the PID controller's settings was intended to increase system performance. Without integrating SMES, we examined several control situations and used stochastic optimization methods (PSO, SCA, and GA) from Section 2.1.2, as illustrated in Fig. 3. Using optimized PSO, SCA and GA algorithms, we ran 50 runs for every parameter modification in order to quantitatively assess the results.

After looking at a number of mutation processes, we carefully documented the related variance, average, best value, worst value, and median ITAE values in Table 4. Our main objectives were to identify the optimal tuning parameters for each of the

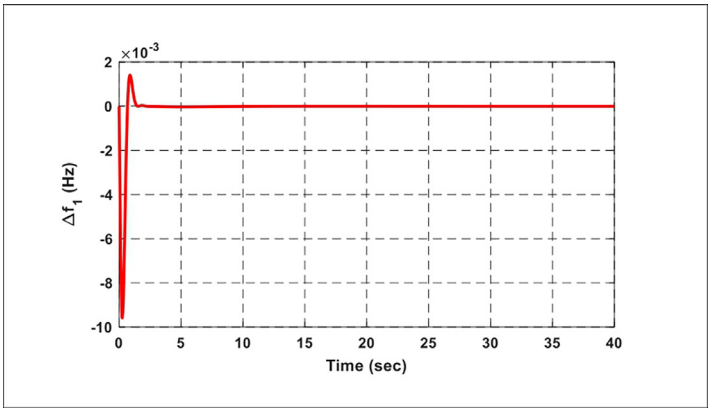

Fig. 8. Frequency shift in Area-1 using parallel AC-DC tie lines.

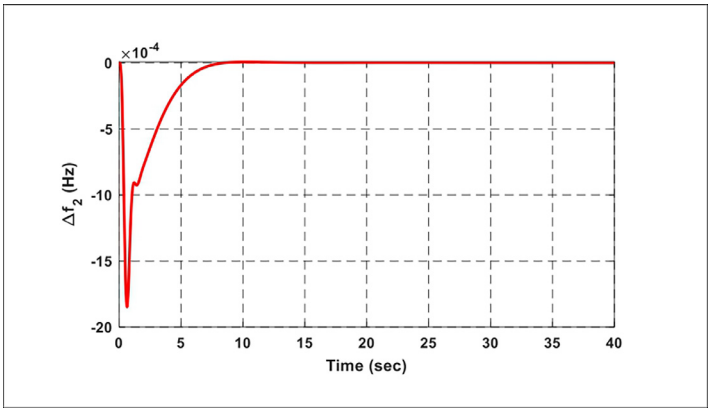

Fig. 9. Variation in frequency in Area-2 with parallel AC-DC tie-lines.

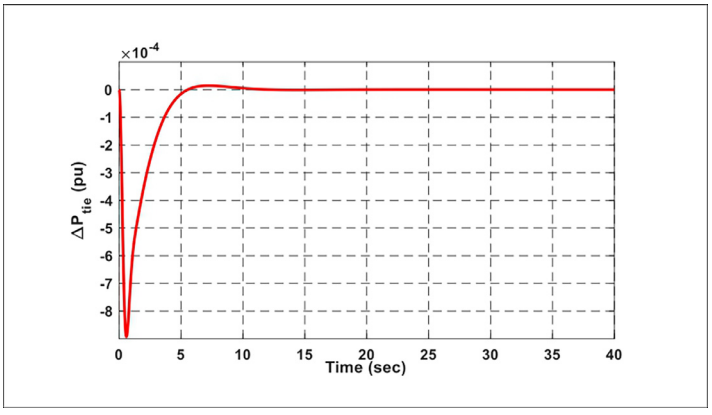

Fig. 10. Variation in tie-line power when using parallel AC-DC tie-lines.

Table 4
Comparison and performance analysis for various stochastic optimization algorithms in multi-source power systems without SMES integration via AC-DC Parallel tie-lines.

Algorithm	Variance	Best value	Worst value	Average value	Mode
PSO	6.2018e−05	0.0310	0.0799	0.0423	0.0310
SCA	5.7268e−06	0.0266	0.0388	0.0316	0.0266
GA	**1.6004e − 05**	0.0324	0.0390	0.0358	0.0324

*Bold fonts indicate the minimum variance of the objective function value.

Table 5
GA tuning results utilizing AC-DC parallel tie-lines without SMES integration for PID controllers and SMES parameters.

Parameters	Value
PID Controller- 1	$K_p1 = 10.000$ $K_i1 = 1.260$ $K_d1 = 1.161$
PID Controller- 2	$K_p2 = 7.609$ $K_i2 = 0.065$ $K_d2 = 0.010$
PID Controller- 3	$K_p3 = 2.055$ $K_i3 = 9.967$ $K_d3 = 0.011$

three PID controllers and to decipher the mechanism that generated them.

To maximize system stability, reduce errors, and achieve desired control goals, an ideal solution consists of balanced PID controller settings. As you can see in Table 5, after 50 iterations of GA, we chose the solution that came closest to meeting our predetermined standards. To ensure effective system control, this solution reflects the ideal combinations of PID controller parameters.

By carefully selecting the optimal tuning parameters from Tables 2 and 5, we can see the effect of those parameters on the multi-

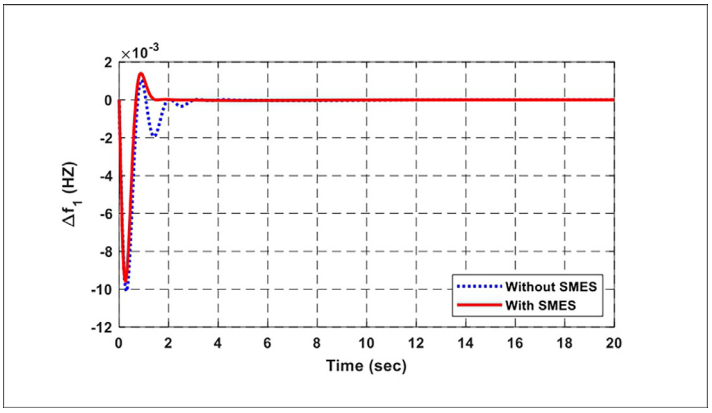

Fig. 11. In a multi-area, multi-source power system, the Area-1 frequency changes both with and without SMES.

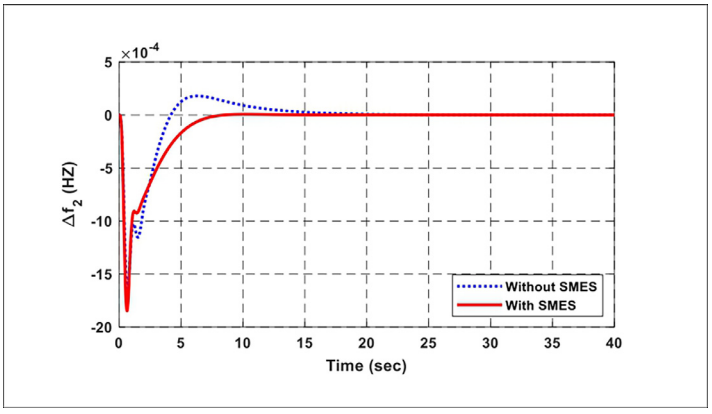

Fig. 12. Variation in Area-2 frequency for multi-area, multi-source power system with and without SMES.

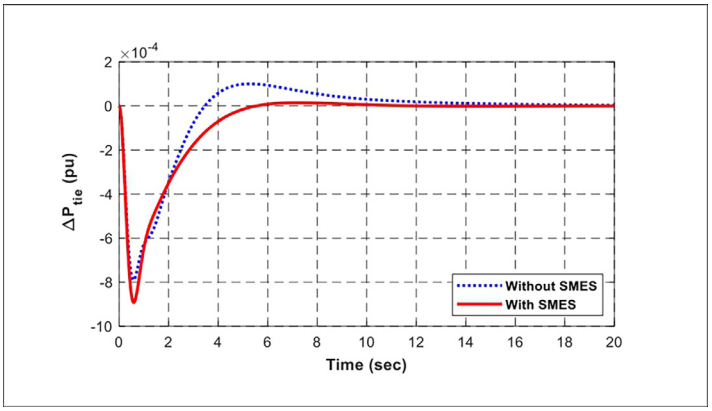

Fig. 13. Tie-line power changes for multi-area, multi-source power systems both with and without SMES.

area, multi-source power system with and without SMES integration. These features have an immediate effect on the performance of the system. Of particular note are the frequencies variations for Areas 1 and 2, respectively, shown in Figs. 11 and 12. Moreover, dynamic fluctuations of the power of the tie-line are depicted in Fig. 13, highlighting the role of AC-DC parallel tie-lines in the overall behavior of the system.

Figure analysis reveals that frequency and tie-line power oscillations settle more slowly in the absence of SMES integration, but the same circumstances settle more quickly when SMES is operational. Furthermore, as Figs. 11–13 illustrates, the results show notable improvements in the minimum damping ratio (MDR), overshoot, and undershoot values. The benefits of SMES integration for system performance are highlighted in these findings.

4.3. Single- and triple-PID controller multi-area multi-source power system

In this study, we exclusively utilize a single PID controller instead of three. The key objective is to enhance the performance of the system by meticulously adjusting the PID controller and the SMES parameters. We employ the ITAE objective function to explore various control scenarios and harness stochastic optimization algorithms (PSO, SCA, and GA) from Section 2.1.2, presented in Fig. 3, while employing only a single PID controller. Our approach entails 50 iterations for each parameter variation using finely tuned PSO, SCA, and GA algorithms, thus quantitatively assessing the outcomes.

Through a systematic analysis of various mutation strategies, we comprehensively document the associated variance, average, best value, worst value, and mode ITAE values in Table 6. Our primary focus remains on identifying the optimal ITAE value and pinpointing the algorithm that offers the most optimal tuning parameters for the singular PID controller and SMES.

Optimal solution attainment hinges on achieving a harmonious blend of balanced PID controller and SMES parameters, aiming to enhance system stability, minimize error, and realize desired control objectives. After subjecting the SCA to 50 iterations, the solution that best aligns with the predefined criteria is selected and presented in Table 7. This

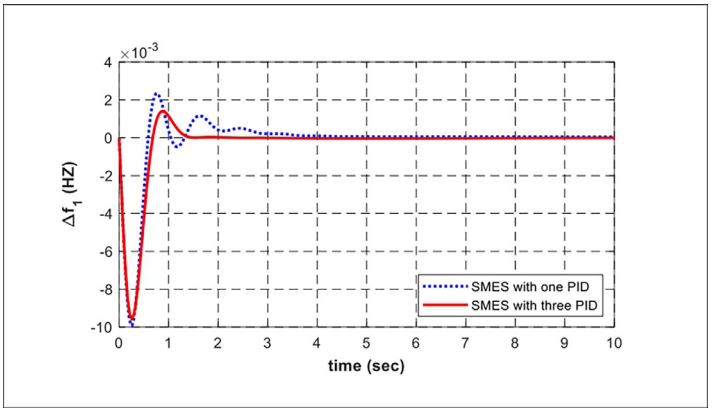

Fig. 14. Variation in Area-1 frequency for multi-area, multi-source power systems using one or three PID controllers.

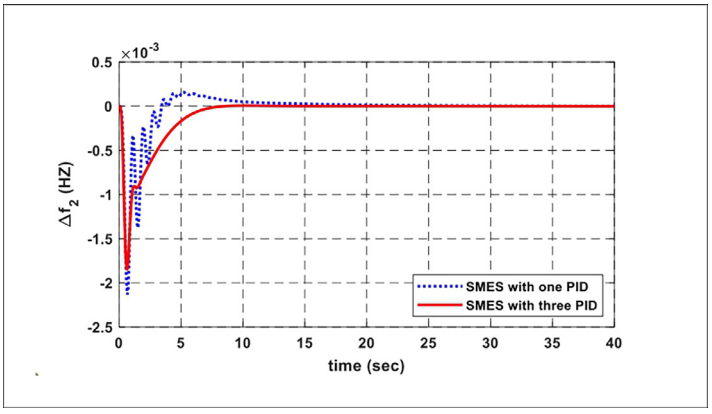

Fig. 15. Change in the Area-2 frequency for a multi-area, multi-source power system using one or more PID controllers.

Table 6
SMES integration through AC-DC parallel tie-lines and comparison and performance study of several stochastic optimization techniques in multi-source power systems with a single PID controller.

Algorithm	Variance	Best value	Worst value	Average value	Mode
PSO	5.3647e−05	0.0315	0.0671	0.0425	0.0310
SCA	6.6903e−06	0.0304	0.0426	0.0328	0.0304
GA	**1.6004e − 05**	0.0310	0.0436	0.0367	0.0315

*Bold fonts indicate the minimum variance of objective function value.

Table 7
SMES integration through AC-DC parallel tie-lines and GA tuning results for PID controller and SMES parameters.

Parameters	Value
PID Controller	Kp = 9.182
	Ki = 9.445
	Kd = 1.111
SMES	k1 = 0.536
	k2 = 5.211
	k3 = 7.654
	k4 = 7.636
	k_$smes$ = 9.765
	t_$smes$ = 0.003

particular solution embodies the finest amalgamation of PID controller and SMES parameters, guaranteeing efficient system control.

The impact of the ideal tuning parameters on the multi-area, multi-source power system with SMES integration is carefully monitored by carefully choosing the ones listed in Tables 2 and 7. In this assessment, the use of one PID controller and the use of three PID controllers are compared. The performance of the system is directly affected by these characteristics. Specifically, Figs. 14 and 15 illustrate frequency fluctuations for Area-1 and Area-2, respectively. Moreover, Fig. 16 highlights the dynamic development of the power of the tie-line, highlighting the critical function that parallel AC-DC tie-lines play in determining the behavior of the system.

Our analysis reveals that oscillations in frequency and tie-line power take longer to stabilize when there is only one PID controller, as opposed to three PID controllers. Furthermore, the figures exhibit notable enhancements in the overshoot, undershoot, and MDR values, as shown in Figs. 14–16. These findings underscore the substantial benefits of SMES integration in system performance.

The comparison given in Table 8 amply demonstrates the beneficial effects of integrating SMES on system performance. Specifically, the table presents the reduced settling times present to the tie-line power, as well as those for Area-1 and Area-2. For Area-1, the settling time increased from 1.7813 to 1.1732; for Area-2, it improved from 6.6671 to 5.8288; and the power of the tie-line improved from 5.0692 to 4.3798. These are particular numerical data. In a similar vein, reduced undershoot values were noted following SMES incorporation.

Even though Area-1's overshoot increased slightly, it was only temporary and stayed within an acceptable range. Improvements with less overshoot were also observed in Area-2 and tie-line power. Additionally, the system with SMES had a smaller area under the curve for the ITAE integral than the one without it. This indicates that the primary goal was achieved, which was to reduce the settling time after SMES integration. Following the incorporation of SMES, the system's overall performance greatly improved.

It is significant to note that three different optimization strategies were used to modify the PID controller's settings. The data clearly show that GA was found to be the most successful in all metrics. Despite the incorporation of SMES, this GA was later used to optimize the PID controller. More precisely, the GA-PID controller generated lower undershoot and overshoot values and shorter settling times, indicating a more responsive and reliable control system.

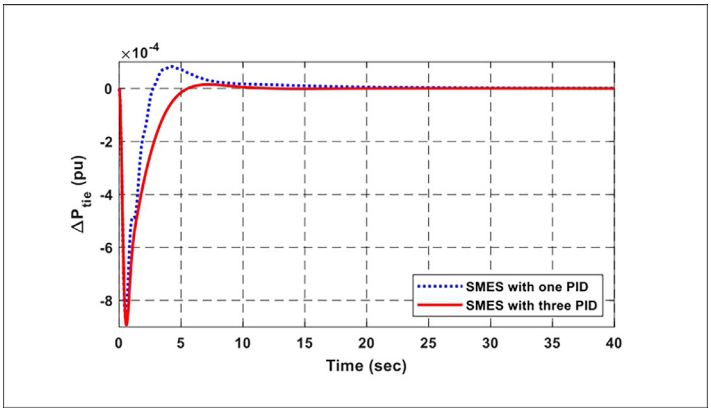

Fig. 16. Tie-line power change for multi-area, multi-source power systems using one or three PID controllers.

Table 8
Control strategy and performance metrics comparison.

Control strategy	Area	Performance metrics		
		Settling time	Overshoot	Undershoot
1 PID controllers with SMES	Area 1 (δ_{f1})	2.4539	0.0023428	0.0099
	Area 2 (δ_{f2})	6.9653	0.0001591	0.0021
	Tie line (δ_{Ptie})	6.2674	0.000084	0.00087
3 PID controllers without SMES	Area 1 (δ_{f1})	1.7813	0.000383	0.0101
	Area 2 (δ_{f2})	6.6671	0.0001796	0.0020
	Tie line (δ_{Ptie})	5.0692	0.0000999	0.0011
3 PID controllers with SMES	Area 1 (δ_{f1})	1.1732	0.001404	0.0096
	Area 2 (δ_{f2})	5.8288	0.0000068	0.0018
	Tie-line (δ_{Ptie})	4.3798	0.0000146	0.00089

Table 9
Investigated cases under system constraint variations.

Case study	Constraint	Initial values		Alteration range	New values	
		Area 1	Area 2		Area 1	Area 2
Parameters variations	B	0.431	0.221	+50 %	0.647	0.332
				+25 %	0.539	0.276
				−25 %	0.323	0.166
				−50 %	0.216	0.111
	R	2.400	2.400	+50 %	3.600	3.600
				+25 %	3.000	3.000
				−25 %	1.800	1.800
				−50 %	1.200	1.200
Load variations	ΔP_D	0.010	0.050	+50 %	0.015	0.075
				+25 %	0.012	0.063
				−25 %	0.007	0.038
				−50 %	0.005	0.025

4.4. Case study

Based upon MATLAB 2022b results, the proposed power network was analyzed into two cases:

- Variations in system parameters in two-area power systems with SMES.
- Change in load within two-area power systems with SMES.

4.4.1. Robustness investigations (case study 1)

The stability of the system is influenced by variability. To handle changes in constraints and ensure resilience, the LFC network requires control actions. In the proposed system, two key parameters that can vary are the frequency bias parameter (B) and the governor speed regulation parameter (R).

Change in frequency bias parameter (B) The resilience of the proposed two-area power system with integrated SMES is evaluated by varying B by ±25 % and ±50 % from its original value while keeping other parameters constant. Table 9 and Figs. 17–19 illustrate the dynamic outcomes.

The frequency response of Area-1 and Area-2 in Figs. 17 and 18, respectively, demonstrate the effect of altering B. Increasing B (+25 % and +50 %) enhances the damping and stability of the system by reducing the overshoot, undershoot and settling time. In contrast, reducing B (−25 % and −50 %) results in less damping,higher oscillations, and delayed settle. The system exhibits robust performance and practical robustness, remaining stable in all circumstances.

ΔP_{tie} is the tie-line power deviation under ±25 % and ±50 % circumstances, as shown in Fig. 19. All situations start off with a sudden and quick reaction that varies in overshoot amplitude. About 15 s later, the system stabilizes. In contrast to the zero and lesser deviations (±25 %), the positive and negative deviations (±50 %) exhibit more oscillations and overshoot. Higher deviations lead to slower settling periods and larger oscillation amplitudes, according to the overall system behavior.

Change in governor speed regulation parameter (R) Variations in parameters affect the stability of the system. To evaluate the robustness of the proposed two-area power system with integrated SMES R it is varied by ±25 % and ±50 % from its original value, while all other parameters remain unchanged. For dynamic findings, see Table 9 and Figs. 20–22.

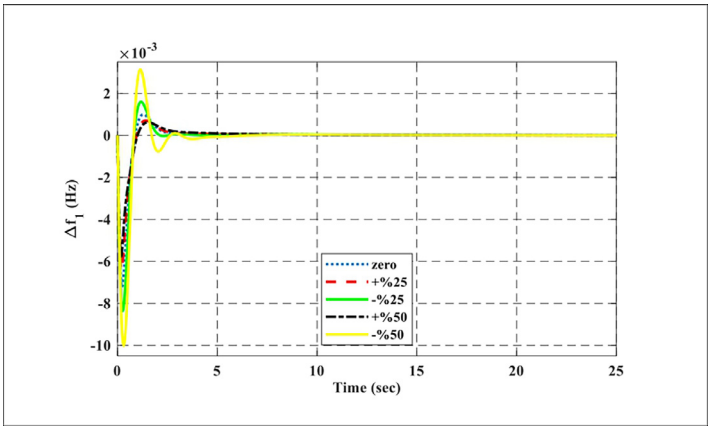

Fig. 17. Frequency response of Area-1 with change in frequency bias parameter (B) while keeping other parameters constant.

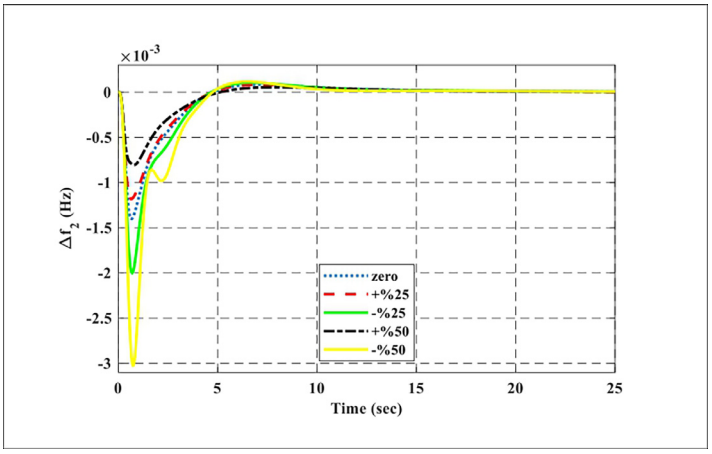

Fig. 18. Frequency response of Area-2 for variation in frequency bias (B), with other parameters unchanged.

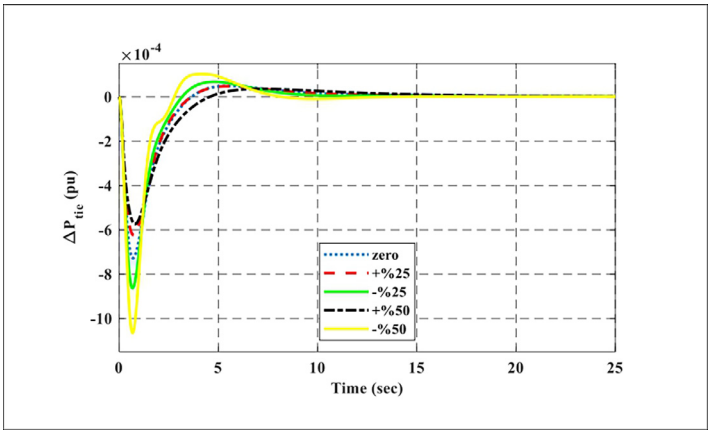

Fig. 19. Tie-line power response for changes in frequency bias (B) with other parameters fixed.

The frequency deviation Δf_1 (in Hz) of Area-1 for changes in the governor speed regulation parameter (R) by ±25 % and ±50 % is shown in Fig. 20. In every instance, the frequency initially rapidly drops before stabilizing in around five seconds. The system eventually recovers to a steady state condition, but the initial divergence increases in size when the parameters are changed more drastically ±50 %. The suggested system, when combined with SMES, shows excellent resilience and robustness to variations in the governor value, as seen by the low oscillations.

Fig. 21 shows the frequency deviation Δf_2 (in Hz) of Area-2 when R varies by ±25 % and ±50 %. The system shows a strong initial frequency decrease followed by a recovery phase. Larger parameter adjustments (+50 % and −50 %) result in a greater divergence, but the system stabilizes in 10 s. The two-area power system integrated with SMES is strong in minimizing disturbances produced by changes in the governor parameter, as seen by the settling time and small overshoot.

Fig. 22 displays the power response of the tie-line (ΔP_{tie}) when R varies by ±25 % and ±50 % from its nominal value. Because of the system's quick reaction to disruptions, there is always an initial undershoot. Its resilience is demonstrated by the system stabilizing in 10 s. Higher deviations are caused by higher R values (+50 %), whereas deeper undershoots are caused by lower values (−50 %). With little effect on stability and settling time, the investigation validates the system's robustness.

4.4.2. Load variations (case study 2)

Fluctuations in load, as indicated in Table 9, were analyzed to test the flexibility of the system.

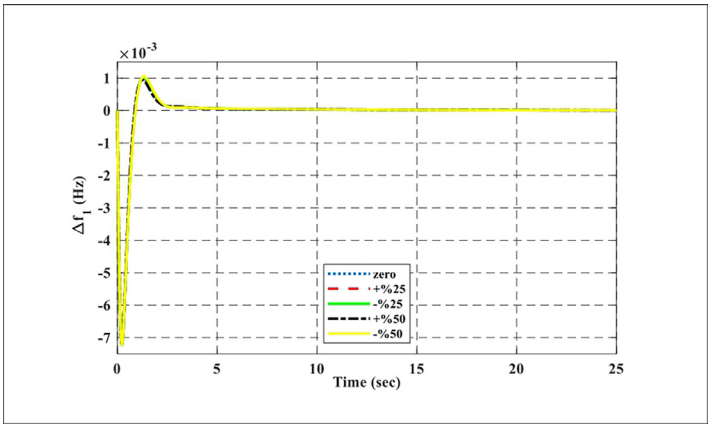

Fig. 20. Frequency response of Area-1 for changes in governor speed regulation parameter (R) with other parameters fixed.

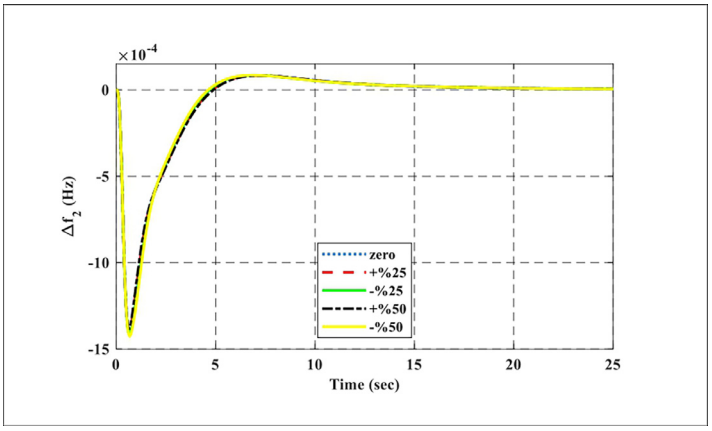

Fig. 21. Area-2 frequency response for variation in governor speed regulation (R) while keeping other parameters constant.

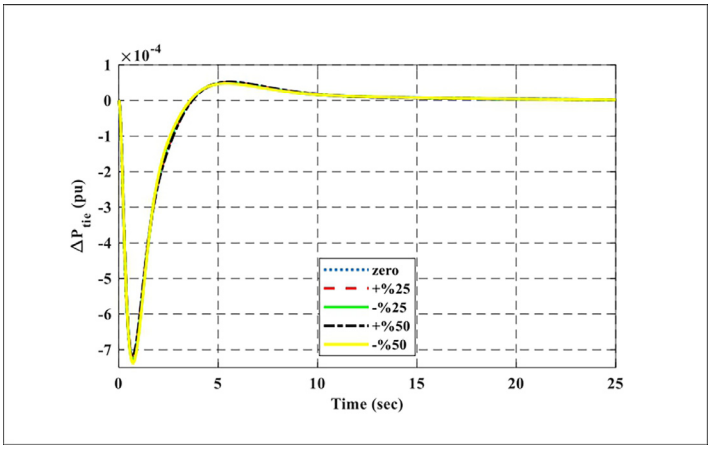

Fig. 22. Tie-line power response (ΔP_{tie}) when governor speed regulation parameter (R) with other parameters fixed.

Fig. 23 illustrates the frequency deviation Δf_1 (in Hz) of Area-1 when the load power ΔP_D changes by ±25 % and ±50 %. The system exhibits a strong initial drop in frequency undershoot followed by damped oscillations before stabilizing. Larger deviations ±50 % cause a greater undershoot and slower recovery. However, the system stabilizes in 8 s, demonstrating robustness and flexibility in handling load disturbances.

Fig. 24 shows the frequency deviation Δf_2 (in Hz) of Area-2 when the load power ΔP_D is varied by ±25 % and ±50 %. A significant initial undershoot is observed, followed by a smooth recovery phase. Larger load deviations (±50 %) cause more pronounced undershoots and slower recovery rates. Despite this, the system stabilizes in 10 s, demonstrating its robustness and flexibility in mitigating load disturbances.

Fig. 25 illustrates the deviation of the power of the tie-line ΔP_{tie} (in pu) under load changes of ±25 % and ±50 %. The system demonstrates an initial sharp undershoot for all scenarios, followed by a recovery phase. The higher deviations (−50 %) result in deeper undershoots, while smaller deviations (+25 %) exhibit minimal oscillations. The system stabilizes in 10 s, showcasing its robustness and ability to handle varying load disturbances.

The proposed study examined the effectiveness of two power system models: a two-area tie-line interconnected power system and a single-area, multi-source power network for LFC. The reactions of these systems to various circumstances, such as variations in the load and parameter values, were examined.

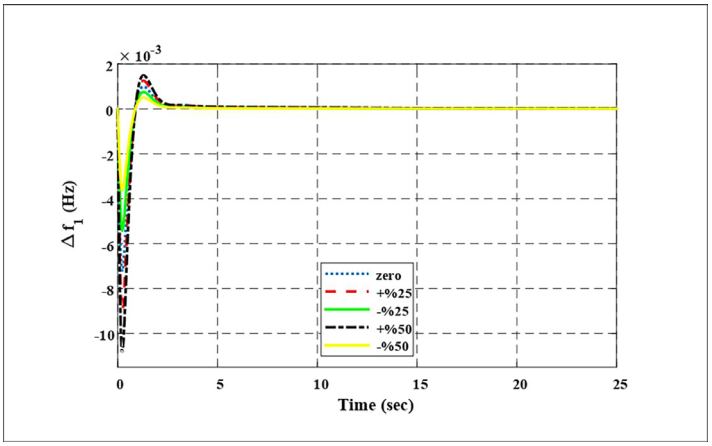

Fig. 23. Frequency response of Area-1 for variations in load power (ΔP_D) with other parameters unchanged.

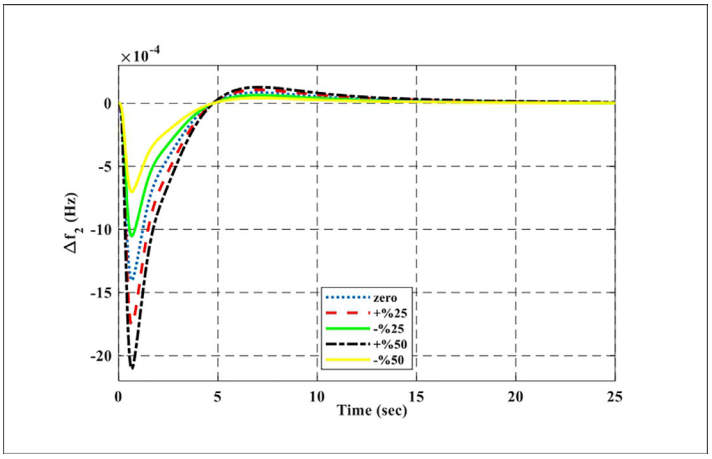

Fig. 24. Frequency response of Area-2 for changes in load power (ΔP_D) while keeping other parameters constant.

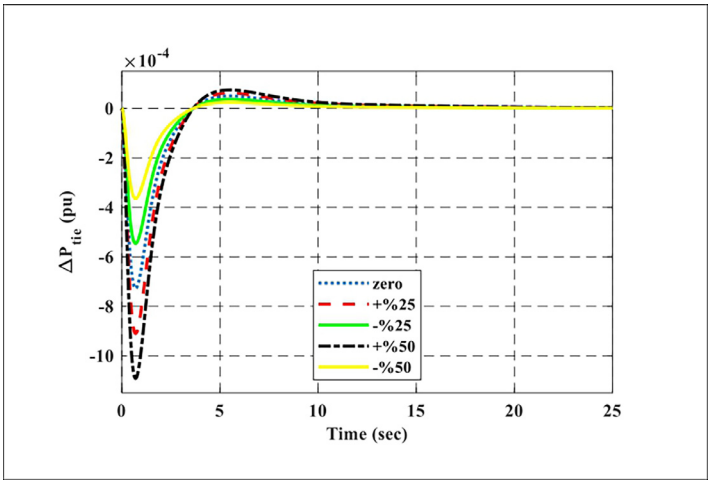

Fig. 25. Tie-line power response for variations in load power (ΔP_D) with other parameters unchanged.

4.5. Stability analysis

The stability analysis is performed in the time domain to assess the robustness of the proposed control strategy. The simulations are executed in MATLAB/SIMULINK, with the controller gain constants and the SMES parameters adjusted for a satisfactory response based on Table 2.

The response in the time domain of the system has been evaluated using the frequency deviation and power deviation responses. The results are derived from the simulation diagram according to the proposed two-area power system with SMES, as shown in Fig. 3. This simulation returns the vector ΔP, which contains t, ΔP_1, ΔP_2, and ΔP_{Tie}.

Fig. 26 illustrates the frequency deviation response of the two-area power system with SMES. The deviations in Area-1 ($\Delta\omega_1$) and Area-2 ($\Delta\omega_2$) are colore red and blue, respectively.

Following a sudden load disturbance, both areas exhibit an initial frequency drop. However, the proposed SMES-based control strategy effectively damps oscillations, ensuring frequency stability. The maximum undershoot for Area-1 reaches approximately -4.8×10^{-3} pu, while Area-2 shows a slightly lower deviation. The oscillations gradually

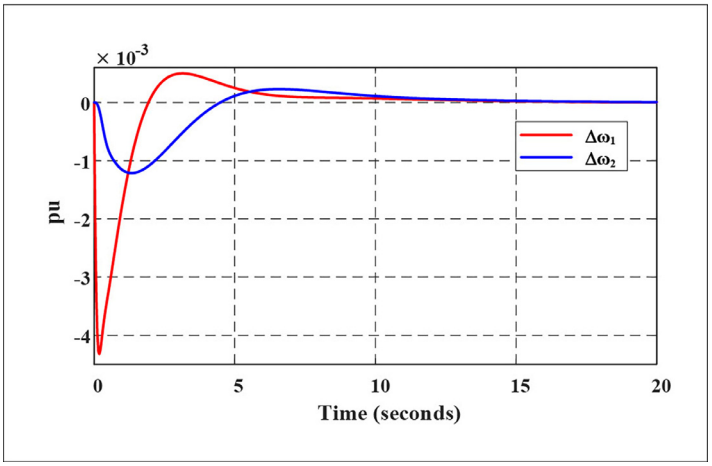

Fig. 26. Step response of frequency deviation for the proposed two-area power system with SMES.

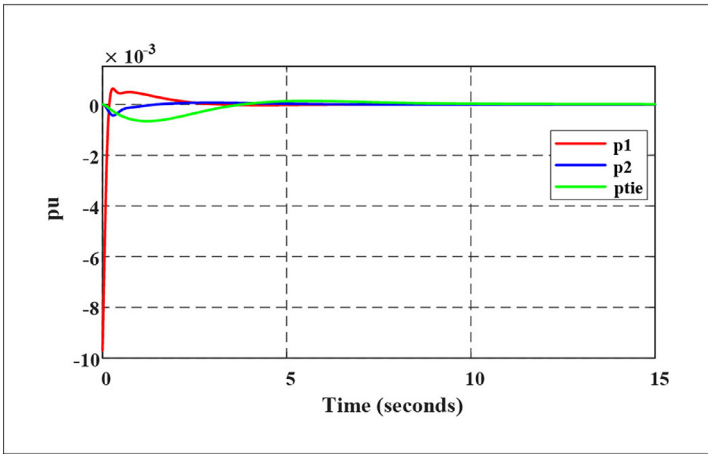

Fig. 27. Step response of power deviation in the proposed two-area power system with SMES integration.

subside and the frequency deviations return to zero with a settling time of around 12–15 s, demonstrating enhanced damping and improved dynamic stability.

Fig. 27 shows how the two-area power system with SMES responds to power variance. The plot is done for the deviations in Area-1 (ΔP_1), Area-2 (ΔP_2), and the power exchange of the tie-line (ΔP_{Tie}).

Initial variations occur after a load disturbance in Area-1; however, the oscillations are successfully dampened by the SMES-based control method. ΔP_{Tie} steadily approaches zero, guaranteeing equitable power distribution throughout the regions. Although ΔP_2 steadily stabilizes with time, ΔP_1 maintains system equilibrium by meeting the growing demand in Area-1.

These outcomes attest to the suggested controller's efficacy in reducing power variations and preserving system stability in dynamic circumstances.

5. Conclusion

A comprehensive study on LFC is presented, focusing on integrating renewable energy sources, conventional generators, and SMES systems. To manage frequency stability and power exchange between interconnected areas, stochastic optimization algorithms such as PSO, GA, and SCA are applied to improve the LFC performance.

In summary, this research emphasizes four critical aspects:

- **SMES-enhanced settling time:** Introducing a PID controller with SMES in each area leads to a significant reduction in settling time. Specifically, in Area-1 (δ_{f1}), the settling time decreases from 2.4539 (without SMES) to 1.1732 (with SMES), representing a notable 34.13 % reduction. However, Area-2 experiences a significant improvement of 12.57 % and the deviation of the power in the tie-line increases by 13.59 % compared to systems without SMES integration. This highlights the accelerated recovery from frequency deviations due to SMES integration.
- **Overshoot reduction:** In the scenario with three PID controllers and SMES, a significant reduction in overshoot is achieved, highlighting the efficacy of the control strategy. Specifically, for Area-1, there is an approximately 73 % reduction. Similarly, for Area-2, a remarkable reduction of about 96 % is observed. Moreover, the power of the tie-line experiences a substantial reduction of approximately 85 %.
- **Undershoot mitigation:** When three PID controllers and SMES, the undershoot for Area-1 is significantly reduced by 5 %, Area-2 is improved by 10 %, and the power of the tie-line is reduced by around 19 %. These percentage-based gains demonstrate how well the control technique reduces the undershoot and strengthens the stability of the power system.
- **Robustness:** The proposed system demonstrates its effectiveness and reliability under dynamic conditions, maintaining performance despite the parameter variations of $\pm 25\,\%$ and $\pm 50\,\%$.
- **System stability:** The proposed SMES-based control strategy enhances dynamic stability by effectively damping frequency and power deviations in a two-area power system.
- **Computational complexity:** The computational burden of LFC is significant when using advanced optimization techniques. This study employs PSO, GA and SCA for PID tuning, where PSO converges

faster, GA incurs higher costs, and SCA balances exploration and exploitation. The integration of SMES further increases computational demand. Despite this, simulation results validate the feasibility of the proposed strategy for real-time applications. Future work may explore hybrid optimization or deep reinforcement learning to improve efficiency and robustness.

In addition, this study thoroughly examines the performance of three PID controllers versus a single PID controller. The analysis reveals valuable insights; the setup with three PID controllers and SMES demonstrates superior performance for this power system. Looking ahead, future investigations should explore fine-tuning the parameters of the SMES system and investigate hybrid approaches that blend different optimization algorithms. This study represents a substantial contribution to the ongoing quest for stable, reliable, and efficient power system operations in an era marked by rapid transformations in energy technologies and sources.

In future work, we will conduct a thorough analysis to address these aspects, including:

- **HIL implementation:** The proposed algorithm will be implemented using Hardware-in-the-Loop (HIL) simulations to evaluate its real-time performance under practical operating conditions, ensuring robustness and accuracy in microgrid or power system environments.
- **Stability analysis:** By employing techniques such as Lyapunov's direct method or frequency domain analysis, we will rigorously assess the stability of the system in different operational scenarios.
- **Robustness evaluation:** We plan to evaluate the resilience of the system to changes in parameters, model uncertainties, and external disturbances. This may involve sensitivity analysis and robustness verification through simulation and experimental validation.

Declaration of competing interest

The authors declare that they have no known competing financial interests or personal relationships that could have appeared to influence the work reported in this paper.

CRediT authorship contribution statement

Md. Shahan Sarker: Conceptualization, Formal analysis, Investigation, Methodology, Software, Resources, Writing – original draft. **Md. Imtiaz Ahmed:** Conceptualization, Methodology, Software, Writing – original draft. **Md. Alamgir Hossain:** Investigation, Methodology, Resources, Supervision, Validation, Writing – review & editing. **Md. Rashidul Islam:** Formal analysis, Investigation, Methodology, Resources, Supervision, Validation, Writing – review & editing. **Md. Arafat Hossain:** Methodology, Software, Writing – original draft. **Md. Rafiqul Islam Sheikh:** Supervision, Validation, Writing – review & editing.

Appendix A. System parameters

The system parameters are as follows: $B1 = 0.4312$ p.u. MW/Hz, $B2 = 0.221$ p.u. MW/Hz, $P_{rt} = 2000$ MW, $P_L = 1840$ MW, $R1 = R2 = R3 = 2.4$ Hz/p.u., $T_{SG} = 0.08$ s, $T_T = 0.3$ s, $K_R = 0.3$, $T_R = 10$ s, $K_{PS1} = K_{PS2} = 68.9566$ Hz/p.u. MW, $T_{PS1} = T_{PS2} = 11.49$ s, $T_{12} = 0.0433$, $a_{12} = -1$, $T_W = 1$ s, $T_{RS} = 5$ s, $T_{RH} = 28.75$ s, $T_{GH} = 0.2$ s, $X_C = 0.6$ s, $Y_C = 1$ s, $c_g = 1$, $b_g = 0.05$ s, $T_F = 0.23$ s, $T_{CR} = 0.01$ s, $T_{CD} = 0.2$ s, $K_T = 0.543478$, $K_H = 0.326084$, $K_G = 0.130438$, $K_{DC} = 1$, $T_{DC} = 0.2$ s.

Appendix B. Algorithm parameters

All algorithm parameters are shown in Table 10.

Table 10
PSO, GA, and SCA Algorithm Operators for Two-area power systems.

Algorithm	Parameters and values
PSO algorithm	
Fitness function	ITAE
Number of variables	Without SMES = 9 With SMES = 15
Number of runs	50
Number of search agents	20
Particle numbers	70
Limit	Lower = 0.01 Upper = 10
$c_1 = c_2$	2
$w_{\max}$	1
$w_{\min}$	0.2
Stopping criteria	Maximum Iterations = 50
SCA Algorithm	
Fitness function	ITAE
Number of variables	Without SMES = 9 With SMES = 15
Number of runs	50
Number of search agents	20
Population size	20
Search space	Lower = 0.01 Upper = 10
Sine-cosine constant (r_1)	[0, 2]
Exploitation parameter (r_2)	Random in [0, 1]
Exploration parameters (r_3, r_4)	Random in [0, 1]
Stopping criteria	Maximum Iterations = 50
Genetic algorithm	
Fitness Function	ITAE
Number of Variables	Without SMES = 9 With SMES = 15
Number of Runs	50
Number of Search Agents	20
Limits	Lower = 0.01 Upper = 10
Population Type	Double Vector
Population Size	20
Creation Function	Random Uniform
Fitness Scaling Function	Rank
Selection Function	Tournament
Crossover Fraction	0.8 (default)
Mutation Function	Random Feasible
Crossover Function	Arithmetic
Stopping Criteria	Maximum Iterations = 50

References

[1] Y. Arya, P. Dahiya, E. Çelik, G. Sharma, H. Gözde, I. Nasiruddin, Agc performance amelioration in multi-area interconnected thermal and thermal-hydro-gas power systems using a novel controller, Eng. Sci. Technol., Int. J. 24 (2) (2021) 384–396.

[2] A.H.A. Elkasem, M. Khamies, M.H. Hassan, A.M. Agwa, S. Kamel, Optimal design of td-ti controller for LFCconsidering renewables penetration by an improved chaos game optimizer, Fractal Fract. 6 (4) (2022) 220.

[3] J. Hasan, M.R. Islam, M.R. Islam, A.Z. Kouzani, M.A.P. Mahmud, A capacitive bridge-type superconducting fault current limiter to improve the transient performance of DFIG/PV/SG-based hybrid power system, IEEE Trans. Appl. Supercond. 31 (8) (2021) 1–5.

[4] M.R. Islam, M.M. Hasan, F.R. Badal, S.K. Das, S.K. Ghosh, A blended improved H5 topology with ilqg controller to augment the performance of microgrid system for grid-connected operations, IEEE Access 8 (2020) 69639–69660.

[5] A. Ameli, A. Hooshyar, E.F. El-Saadany, A.M. Youssef, Attack detection and identification for automatic generation control systems, IEEE Trans. Power Syst. 33 (5) (2018) 4760–4774.

[6] R. Mohammadikia, M. Aliasghary, A fractional order fuzzy pid for load frequency control of four-area interconnected power system using biogeography-based optimization, Int. Trans. Electr. Energy Syst. 29 (2) (2019) e2735.

[7] M.Y.-Y.U. Haque, M.R. Islam, T. Ahmed, M.R.I. Sheikh, Improved voltage tracking of autonomous microgrid technology using a combined resonant controller with lead--lag compensator adopting negative imaginary theorem, Prot. Control Mod. Power Syst. 7 (1) (2022) 1–16.

[8] T. Ali, S.A. Malik, I.A. Hameed, A. Daraz, H. Mujlid, A.T. Azar, Load frequency control and automatic voltage regulation in a multi-area interconnected power system using nature-inspired computation based control methodology, Sustainability 14 (19) (2022) 12162.

[9] T. Ali, S.A. Malik, A. Daraz, S. Aslam, T. Alkhalifah, Dandelion optimizer-based combined automatic voltage regulation and load frequency control in a multi-area, multi-source interconnected power system with nonlinearities, Energies 15 (22) (2022) 8499.

[10] M.A. Metwally, M.A. Ali, S.A. Kutb, F.M. Bendary, A genetic algorithm for optimum design of pid controller in multi area load frequency control for egyptian electrical grid, Int. J. Eng. Res. Technol. 5 (10) (2016).

[11] Ibraheem, P. Kumar, D.P. Kothari, Recent philosophies of automatic generation control strategies in power systems, IEEE Trans. Power Syst. 20 (2005) 346–357.

[12] X. Zhang, C. Deng, P. Cao, Z. Long, Regional decentralized coordinated AGC based on hierarchical model predictive control, Electr. Power Syst. Res. 225 (2023) 109779.

[13] R. Kannan, J.R. Luedtke, L.A. Roald, Stochastic DC optimal power flow with reserve saturation, Electr. Power Syst. Res. 189 (2020) 106566.

[14] B. Mohanty, S. Panda, P. Hota, Controller parameters tuning of differential evolution algorithm and its application to load frequency control of multi-source power system, Int. J. Electr. Power Energy Syst. 54 (2014) 77–85.

[15] H. Park, R. Baldick, Optimal capacity planning of generation system integrating uncertain solar and wind energy with seasonal variability, Electr. Power Syst. Res. 180 (2020) 106072.

[16] M.R. Islam, J. Hasan, M.R. Islam, A.Z. Kouzani, M.P. Mahmud, Transient performance augmentation of DFIG based wind farms by nonlinear control of flux-coupling-type superconducting fault current limiter, IEEE Trans. Appl. Supercond. 31 (8) (2021) 1–5.

[17] J. Smith, E. Johnson, A. Ali, Adjusting load in distinct scenarios for double-area tie-line power systems using optimized pid controllers, Int. J. Electr. Power Energy Syst. 142 (2024) 108234.

[18] N.R. Babu, S.K. Bhagat, L.C. Saikia, T. Chiranjeevi, R. Devarapalli, F.P.G. Márquez, A comprehensive review of recent strategies on automatic generation control/load frequency control in power systems, Arch. Comput. Methods Eng. 30 (1) (2023) 543–572.

[19] Y.-Q. Bao, Y. Li, B. Wang, M. Hu, P. Chen, Demand response for frequency control of multi-area power system, J. Mod. Power Syst. Clean Energy 5 (1) (2017).

[20] M.A. Hossain, M.R. Islam, M.Y.-Y.U. Haque, J. Hasan, T.K. Roy, M.A.H. Sadi, Protecting DFIG-based multi-machine power system under transient-state by nonlinear adaptive backstepping controller-based capacitive BFCL, IET Gener., Transm. Distrib. 16 (22) (2022) 4528–4548.

[21] A. Prakash, S. Murali, R. Shankar, R. Bhushan, HVDC tie-link modeling for restructured AGC using a novel fractional order cascade controller, Electr. Power Syst. Res. 170 (2019) 244–258.

[22] K. Singh, Y. Arya, Jaya-itdf control strategy-based frequency regulation of multi-microgrid utilizing energy stored in high-voltage direct current-link capacitors, Soft Comput. 27 (2023) 5951–5970.

[23] S. Rajamand, Load frequency control and dynamic response improvement using energy storage and modeling of uncertainty in renewable distributed generators, J. Energy Storage 37 (2021) 102467.

[24] X.-C. Shangguan, C.-K. Zhang, Y. He, L. Jin, L. Jiang, J.W. Spencer, M. Wu, Robust load frequency control for power system considering transmission delay and sampling period, IEEE Trans. Ind. Inf. 17 (8) (2020) 5292–5303.

[25] N. Hakimuddin, A. Khosla, J.K. Garg, Comparative performance investigation of genetic algorithms (GAS), particle swarm optimization (PSO), and bacteria foraging algorithm (BFA) based automatic generation control (AGC) with multi source power plants (MSPPS), Electr. Power Compon. Syst. 49 (2022) 1–12.

[26] S. Chaine, M. Tripathy, Design of an optimal smes for automatic generation control of two-area thermal power system using cuckoo search algorithm, J. Electr. Syst. Inf. Technol. 2 (1) (2015) 1–13.

[27] M.R. Islam, D.D. Abir, M.R. Islam, J. Hasan, M.N. Huda, K.M. Muttaqi, D. Sutanto, Enhancement of frt capability of dfig based wind farm by a hybrid superconducting fault current limiter with bias magnetic field, in: 2020 IEEE International Conference on Power Electronics, Smart Grid and Renewable Energy (PESGRE2020), 2020, pp. 1–6.

[28] B. Mohanty, S. Panda, P. Hota, Controller parameters tuning of differential evolution algorithm and its application to load frequency control of multi-source power system, Int. J. Electr. Power Energy Syst. 54 (2014) 77–85.

[29] M.-P. Song, G.-C. Gu, Research on particle swarm optimization: a review, in: Proceedings of 2004 International Conference on Machine Learning and Cybernetics (IEEE Cat. No.04EX826), 4, 2004, pp. 2236–2241.

[30] M. Srinivas, L. Patnaik, Genetic algorithms: a survey, Computer 27 (6) (1994) 17–26.

[31] A.I. Abeg, M.R. Islam, M.A. Hossain, M.F. Ishraque, M.R. Islam, M. Hossain, Capacity and operation optimization of hybrid microgrid for economic zone using a novel meta-heuristic algorithm, J. Energy Storage 94 (2024) 112314.

[32] A.I. Hafez, H.M. Zawbaa, E. Emary, A.E. Hassanien, Sine cosine optimization algorithm for feature selection, in: 2016 International Symposium on INnovations in Intelligent SysTems and Applications (INISTA), 2016, pp. 1–5.

[33] A.K. Barisal, Comparative performance analysis of teaching learning based optimization for automatic load frequency control of multi-source power systems, Int. J. Electr. Power Energy Syst. 66 (2014) 67–77.

[34] T.K. Mohapatra, A.K. Dey, B.K. Sahu, Employment of quasi oppositional ssa-based two-degree-of-freedom fractional order pid controller for AGC of assorted source of generations, IET Gener., Transm. Distrib. 14 (19) (2020) 4291–4303.

[35] M.V. Mahendran, V. Vijayan, Model-predictive control-based hybrid optimized load frequency control of multi-area power systems, IET Gener., Transm. Distrib. 15 (19) (2021) 4291–4303.

[36] V. Rameshar, G. Sharma, P.N. Bokoro, E. Çelik, Frequency support studies of a diesel-wind generation system using snake optimizer-oriented pid with uc and rfb, Energies 16 (8) (2023) 1–20.

[37] Y. Abdel-Magid, M. Abido, Agc tuning of interconnected reheat thermal systems with particle swarm optimization, in: Proceedings of the 2003 10th IEEE International Conference on Electronics, Circuits and Systems, 1, 2003, pp. 376–379.

[38] K.P.S. Parmar, S. Majhi, D.P. Kothari, Improvement of dynamic performance of LFC of the two area power system: an analysis using matlab, Int. J. Comput. Appl. 40 (2012) 28–32.

[39] A. Haghrah, B. Mohammadi-Ivatloo, S. Seyedmonir, Real coded genetic algorithm approach with random transfer vectors-based mutation for short-term hydro-thermal scheduling, IET Gener., Transm. Distrib. 9 (2) (2015) 168–178.

[40] V. Jeyalakshmi, P. Subburaj, Pso-scaled fuzzy logic to load frequency control in hydrothermal power system, Soft Comput. 20 (2016) 2577–2594.

[41] M. Elsisi, M. Aboelela, M. Soliman, W. Mansour, Design of optimal model predictive controller for LFCof nonlinear multi-area power system with energy storage devices, Electr. Power Compon. Syst. 46 (11–12) (2018) 1300–1311.

[42] P.N. Topno, S. Chanana, Load frequency control of a two-area multi-source power system using a tilt integral derivative controller, J. Vib. Control 24 (1) (2018) 110–125.

[43] A. Kumar, S. Suhag, Effect of tcps, smes, and DFIG on load frequency control of a multi-area multi-source power system using multi-verse optimized fuzzy-pid controller with derivative filter, J. Vib. Control 24 (24) (2018) 5922–5937.

[44] T. Jena, M.K. Debnath, S.K. Sanyal, Optimal fuzzy-pid controller with derivative filter for load frequency control including upfc and smes, Int. J. Electr. Comput. Eng. 9 (4) (2019) 2813.

[45] A. Prakash, S. Murali, R. Shankar, R. Bhushan, HVDC tie-link modeling for restructured AGC using a novel fractional order cascade controller, Electr. Power Syst. Res. 170 (2019) 244–258.

[46] H.H. Ali, A.M. Kassem, M. Dhaifullah, A. Fathy, Multi-verse optimizer for model predictive load frequency control of hybrid multi-interconnected plants comprising renewable energy, IEEE Access PP (99) (2020) 1.

[47] M.R. Islam, J. Hasan, M.R.R. Shipon, M.A.H. Sadi, A. Abuhussein, T.K. Roy, Neuro fuzzy logic controlled parallel resonance type fault current limiter to improve the fault ride through capability of DFIG-based wind farm, IEEE Access 8 (2020) 115314–115334.

[48] C.N.S. Kalyan, B.S. Goud, C.R. Reddy, H.S. Ramadan, M. Bajaj, Z.M. Ali, Water cycle algorithm optimized type II fuzzy controller for load frequency control of a multi-area, multi-fuel system with communication time delays, Energies 14 (17) (2021) 5387.

[49] E. Çelik, N. Ozturk, E. Houssein, Improved load frequency control of interconnected power systems using energy storage devices and a new cost function, Neural Comput. Appl. 34 (2022) 17439–17457.

[50] A. Singh, V. Kumar, P. Sharma, A hybrid genetic algorithm and particle swarm optimization approach for load frequency control of a multi-area power system, Energy Rep. 9 (2023) 256–267.

[51] E. Çelik, Others, Performance analysis of ssa optimized fuzzy 1PD-PI controller on AGC of renewable energy assisted thermal and hydro-thermal power systems, J. Ambient Intell. Humaniz. Comput. 13 (8) (2022) 4103–4122.

[52] E. Çelik, N. Öztürk, Novel fuzzy 1pd-ti controller for AGC of interconnected electric power systems with renewable power generation and energy storage devices, Eng. Sci. Technol., Int. J. 35 (2022) 101166.

[53] J. Khalid, M.A.M. Ramli, M.S. Khan, T. Hidayat, Efficient load frequency control of renewable integrated power system: a twin delayed ddpg-based deep reinforcement learning approach, IEEE Access 10 (2022) 51561–51574.

[54] S.D. Al-Majidi, M.K. AL-Nussairi, A.J. Mohammed, A.M. Dakhil, M.F. Abbod, H.S. Al-Raweshidy, Design of a load frequency controller based on an optimal neural network, Energies 15 (2022) 6223.

[55] N.R. Babu, S.K. Bhagat, L.C. Saikia, T. Chiranjeevi, R. Devarapalli, F.P.G. Márquez, A comprehensive review of recent strategies on automatic generation control/load frequency control in power systems, Arch. Comput. Methods Eng. 30 (1) (2023) 543–572.

[56] N. Nayak, S. Mishra, D. Sharma, B.K. Sahu, Application of modified sine cosine algorithm to optimally design pid/fuzzy-pid controllers to deal with AGC issues in deregulated power system, IET Gener., Transm. Distrib. 13 (12) (2019) 2474–2487.

[57] N.R. Babu, T. Chiranjeevi, A. Saha, S.K. Bhagat, Comparative analysis of various energy storage systems in a conventional LFC system considering rdsts, pwts and ahvdc models, J. Eng. Res. 11 (4) (2023) 425–436.

[58] J. Zahariah, T.P.V. Symon, Analysis of multiple-area renewable integrated hydro-thermal system considering artificial rabbit optimized pi (fopd) cascade controller and redox flow battery, Arch. Control Sci. 22 (2023) 861–884.

[59] N.R. Babu, T. Chiranjeevi, R. Devarapalli, S.K. Bhagat, Optimal location of facts devices in LFC studies considering the application of rt-lab studies and emperor penguin optimization algorithm, J. Eng. Res. 11 (2) (2023) 100060.

[60] N. Ram Babu, T. Chiranjeevi, R. Devarapalli, L. Knypiński, F.P. García Márquez, Real-time validation of an automatic generation control system considering hpa-ise with crow search algorithm optimized cascade FOPDN-FOPIDN controller, Arch. Control Sci. 33 (2023) 371–390.

[61] W. Bahloul, M. Chtourou, M.B. Ammar, H.H. Abdallah, Robust neural controllers for power system based on new reduced models, Adv. Electr. Electron. Eng. 21 (2023) 13.

[62] N.R. Babu, T. Chiranjeevi, A. Saha, Application of rt-lab in multi-area AGC system under deregulated environment considering ipfc-smes, Iran. J. Sci. Technol., Trans. Electr. Eng. 48 (4) (2024) 1643–1656.

[63] E. Çelik, Exponential pid controller for effective load frequency regulation of electric power systems, ISA Trans. 153 (2024) 364–383.

[64] S. Masikana, G. Sharma, S. Sharma, P.N. Bokoro, E. Çelik, Solar PV focused LFC studies utilizing an sfs-optimized pid with fractional derivative (pidd$_\mu$), and incorporating bess and fess applications, e-Prime - Adv. Electr. Eng., Electron. Energy 10 (2024) 100787.

[65] A. Saha, P. Dash, T. Chiranjeevi, N.R. Babu, Implementation of combined hydrogen aqua electrolyser-fuel cell and redox-flow-battery under restructured situation of AGC employing TSA optimized PDN(FOPI) controller, J. Taibah Univ. Sci. 18 (1) (2024) 2334004.

[66] Z. Liu, H. Wang, J. Li, X. Zhang, Reinforcement learning-based approach for load frequency control in power systems with high penetration of renewables, Energy Rep. 9 (2023) 102–113.
[67] J. Zahariah, T.P.S.V. A, Hybrid aquila arithmetic optimization based anfis for harmonic mitigation in grid connected solar fed distributed energy systems, Electr. Power Syst. Res. 226 (2024) 109898.
[68] Z. Qu, W. Younis, X. Liu, A.K. Junejo, S.Z. Almutairi, P. Wang, Optimized pid controller for load frequency control in multi-source and dual-area power systems using pso and ga algorithms, IEEE Access (2024). This study is supported via funding from Prince Sattam bin Abdulaziz University, project number (PSAU/2024/R/1445).
[69] R. Sharma, N. Gupta, V. Kumar, Firefly algorithm for load frequency control optimization in multi-area power systems, Int. J. Electr. Power Energy Syst. 120 (2020) 105975.
[70] K.V. A. Kumar S. Singh, Artificial bee colony optimization for pid controller in load frequency control of power systems, Int. J. Emerg. Electr. Power Syst. 22 (5) (2021) 495–512.
[71] K. Singh, Y. Arya, Tidal turbine support in microgrid frequency regulation through novel cascade fuzzy-FOPID droop in de-loaded region, ISA Trans. 133 (2023) 218–232.
[72] K. Peddakapu, P. Srinivasarao, M. Mohamed, Y. Arya, D.K. Kishore, Stabilization of frequency in multi-microgrid system using barnacle mating optimizer-based cascade controllers, Sustain. Energy Technol. Assess. 54 (2022) 102823.
[73] R. Choudhary, J. Rai, Y. Arya, FOPTID + 1 controller with capacitive energy storage for AGC performance enrichment of multi-source electric power systems, Electr. Power Syst. Res. 221 (2023) 109450.